Horizontal distributions of aerosol constituents and their mixing states in Antarctica during the JASE traverse

K. Hara[1], F. Nakazawa[2], S. Fujita[2], K. Fukui[2, now at 3], H. Enomoto[4, now at 2], and S. Sugiyama[5]

1: Department of Earth System Science, Faculty of Science, Fukuoka University, Fukuoka, Japan

2: National Institute of Polar Research, Tokyo, Japan

3: Tateyama Caldera Sabo Museum, Toyama, Japan

4: Kitami Institute of Technology, Kitami, Japan

5: Institute of Low temperature Science, Hokkaido University, Sapporo, Japan

Submitted to ACP

Abstract

Measurements of aerosol number concentrations and direct aerosol sampling were conducted on continental Antarctica during the traverse of the Japanese–Swedish joint Antarctic expedition (JASE) from 14 November 2007 until 24 January 2008. Aerosol concentrations in background conditions decreased gradually with latitude in inland regions during the traverse. The lowest aerosol number concentrations were 160 L^{-1} in $D_p > 0.3$ μm, and 0.5 L^{-1} in $D_p > 2$ μm. In contrast, aerosol concentrations reached 3278 L^{-1} in $D_p > 0.3$ μm, and 215 L^{-1} in $D_p > 2$ μm under strong wind conditions. The estimated aerosol mass concentrations were 0.04–5.7 μg m^{-3}. Single particle analysis of aerosol particles collected during the JASE traverse was conducted using a scanning electron microscope equipped with an energy dispersive X-ray spectrometer. Major aerosol constituents were sulfates in fine mode, and sulfate, sea-salts, modified sea-salts, and fractionated sea-salts in coarse mode. K-rich sulfates, Mg-rich sulfate, Ca-rich sulfates, and minerals were identified as minor aerosol constituents. Horizontal features of Cl/Na ratios imply that sea-salt modification (i.e. Cl loss) occurred on the Antarctic continent during the summer. Most sea-salt particles in the continental region near the coast were modified with acidic sulfur species such as SO_4^{2-} and $CH_3SO_3^-$. By contrast, acidic species other than the acidic sulfur species (likely NO_3^-) contributed markedly to sea-salt modification in inland areas during the traverse. Mg-rich sea-salt particles and Mg-free sea-salt particles were present in coarse and fine modes from the coast to inland

41 areas. These sea-salt particles might be associated with sea-salt fractionation on the
42 snow surface of continental Antarctica.

1 Introduction

Atmospheric aerosol constituents in Antarctic regions have been measured for more than three decades to elucidate the regions' aerosol chemistry, to monitor Earth background levels, and to interpret ice core records (Savoie et al., 1992, 1993; Minikin et al., 1998; Legrand et al., 2001; Hara et al., 2004; Weller et al., 2011). Although most investigations of aerosol chemistry have been conducted at coastal stations such as Syowa Station, Neumayer Station, Halley Station, Dumont d'Urville Station, and Mawson Station (Savoie et al., 1992, 1993; Legrand et al., 2001; Hara et al., 2004; Weller et al., 2011), aerosol chemistry and atmospheric chemistry have been investigated recently even at inland stations such as Amundsen–Scott (South Pole) Station, Dome F Station, Kohnen Station, and Concordia (Dome C) Station (Bodhaine, 1995; Hara et al., 2004; Weller and Wagenbach, 2007; Jourdain et al., 2008; Eisele et al., 2008; Udisti et al., 2012).

From those earlier investigations, basic aerosol chemical properties were obtained: seasonal features of the concentrations of major aerosol constituents (SO_4^{2-}, $CH_3SO_3^-$, NO_3^-, and sea-salts (e.g., Na^+ and Cl^-)), and minor aerosol constituents (minerals and carbonaceous species (soot and organics)) at Antarctic coasts and inland area. In those investigations, aerosol constituents were determined using bulk analysis techniques (mainly ion chromatography). Such techniques, however, cannot provide sufficient

63 information about the mixing states of respective aerosol constituents. That information
64 is necessary to elucidate the origins of constituents and the chemical reactions that occur
65 on aerosol particles (heterogeneous reactions). For sample analysis, single particle
66 analysis takes longer than bulk analysis. Therefore, few previous investigations have
67 used single particle analysis (Parungo et al., 1979; Yamato et al., 1987a, 1987b; Artaxo
68 et al., 1992; Mouri et al., 1999; Hara et al., 1996, 2005, 2013).
69
70 Previous investigations (e.g., Savoie et al., 1992, 1993; Minikin et al., 1998; Hara et al.,
71 2004, 2013) showed that major aerosol constituents in Antarctic atmosphere near
72 surface were sulfates (probably H_2SO_4) in summer and sea-salts in winter–spring.
73 Actually, SO_4^{2-} and $CH_3SO_3^-$ are strongly dominant during the summer on the
74 Antarctica because of biogenic activity in the ocean (e.g., Minikin et al., 1998; Legrand
75 et al., 2001). Size segregated aerosol analysis showed that SO_4^{2-} and $CH_3SO_3^-$ were
76 distributed mainly in the sub-micrometer range at the Antarctic coasts (e.g., Jourdain
77 and Legrand, 2001; Read et al., 2008). Yamato et al. (1987a, 1987b) used chemical
78 testing (Ca thin-film method) to demonstrate that sulfuric acid was dominant in aerosol
79 constituents in Antarctic troposphere during summer. In addition, single particle
80 analysis using laser microprobe mass spectrometry showed that $CH_3SO_3^-$ was mixed
81 internally with sulfate particles (probably H_2SO_4 particles) near the surface on the
82 Antarctic coasts during summer (Wouters et al., 1990; Hara et al., 1995).

Sea-salts are dominant during winter–spring (e.g., Hara et al., 2004). Sea-salt particles were distributed widely in ultrafine–coarse mode throughout the year at Syowa Station (Hara et al., 2010a, 2011a) and were distributed in fine–coarse mode during the summer at Aboa Station (Kerminen et al., 2000; Teinilä et al., 2000). From elemental analysis of individual particles using EDX, Mouri et al. (1999) and Hara et al. (2005, 2013) reported that sea-salt particles near the surface were modified with SO_4^{2-} and $CH_3SO_3^-$ during the summer, and were modified with NO_3^- in August at Syowa Station. Furthermore, single particle analysis of aerosol particles collected using tethered-balloon operations exhibited seasonal and vertical features of aerosol constituents and their mixing states in near surface – lower free troposphere (2.5 km), sea-salt modification, and sea-salt fractionation (Hara et al., 2013). In addition to sea-salt modification, sea-salt particles were fractionated through precipitation of several salts such as mirabilite (Na_2SO_4 $10H_2O$) and hydrohalite (NaCl $2H_2O$) in sea ice formation and frost flower appearance under colder conditions (e.g., Wagenbach et al., 1998; Rankin et al., 2000, 2002; Hara et al., 2004, 2012). Sea-salt fractionation on sea ice (including frost flowers) by depletion of Na-salts engenders Mg-enrichment in sea-salt particles during winter–spring on the Antarctic coast (Hara et al., 2010, 2012, 2013). Furthermore, Hara et al. (2013) pointed out the likelihood that sea-salt fractionation (Mg separation in sea-salt particles) occurs during summer. The following questions,

however, remain; (1) “Where does sea-salt fractionation occur on the Antarctic regions during summer?”, and (2) “What are the specific processes of sea-salt fractionation (Mg separation)?”.

Although useful and important knowledge related to aerosol chemical properties (e.g., concentrations, and mixing states) has been obtained gradually from previous investigations using bulk and single-particle analysis of aerosol particles along the Antarctic coasts, a great dearth of knowledge remains for aerosol chemical properties and chemical processes taking place on the Antarctic continent. To elucidate spatiotemporal features of glaciological environment and atmospheric quality in Droning Maud Land, East Antarctica, scientific traverse using snow vehicles was conducted by a Japanese Swedish Antarctic Expedition (JASE) in the austral summer of 2007/2008 (Fujita et al., 2011). In this study, measurements of the aerosol number concentrations and direct aerosol sampling were conducted during the JASE traverse to characterize and elucidate the horizontal features of aerosol constituents and their mixing states in the atmosphere near the ground on the Antarctic continent during summer. Herein, we mainly discuss (1) the horizontal distributions of aerosol constituents and mixing states on the Antarctic continent during summer, (2) sea-salt modification, and (3) sea-salt fractionation.

2 Aerosol measurements and data analysis

2-1 JASE traverse

Figure 1 depicts the JASE traverse route in Droning Maud Land, East Antarctica. On this campaign, the Japanese team traveled from S16 on the Antarctic continent (near Syowa Station) to a meeting point on the Antarctic plateau via Dome F Station. The Swedish team traveled from Wasa Station to the meeting point via Kohnen Station. Aerosol measurements and direct aerosol sampling for this study were conducted during the Japanese team traverse. The Japanese traverse team left from S16 on 14 November 2007, and arrived at the meeting point on 27 December 2007 in the incoming traverse. After some joint scientific work at the meeting point conducted for several days, the outgoing traverse (return to S16) began on 30 December 2007. During the outgoing traverse, the Japanese team traveled from the meeting point to Dome F on the southern side of the ice divide for glaciological measurements. The team approached S16 on 24 January 2008. Details of the traverse were described by Fujita et al. (2011).

2-2 Meteorological measurements during the JASE traverse

Continuous measurements of air pressure (F4711; Yokogawa Analytical Systems Inc.), air temperature (KDC-A01-S001 and KADEC21-U4; Kona System Inc.), wind speed, and wind direction (KADEC21-KAZE; Kona System Inc.) were performed during the JASE traverse. Meteorological sensors were fixed on the snow vehicle, located

143 approximately at 3 m above the snow surface. Daily meteorological observations (air,
144 pressure, air temperature, wind direction, wind speed, weather, visibility, degree of
145 cloud cover, and cloud type) were made around 15:00 LT. Weather conditions were
146 observed also during aerosol measurements conducted at camp sites.
147
148 **2-3 Aerosol measurements**
149 Aerosol measurements and direct aerosol sampling were conducted during the JASE
150 traverse. For safe operation of aerosol measurements, measurements of the aerosol size
151 distribution, and direct aerosol sampling were not made during the traverse during the
152 daytime but were conducted only at camp sites.
153
154 **2-3-1 Measurements of aerosol number concentrations**
155 Aerosol number concentrations were measured using a portable optical particle counter
156 (OPC, KR12A; Rion Co. Ltd.) during direct aerosol sampling at every camp site. The
157 measurable size range was D_p> 0.3, 0.5, 0.7, 1.0, 2.0, and 5.0 μm. The OPC was
158 calibrated using spherical polystyrene latex particles with refractive index of 1.59–0i.
159 Consequently, the size provided from OPC is "optically PSL-equivalent size". The OPC
160 packed in an insulator box was set at ca. 1 m above the snow surface by tripod, located
161 on the windward side of the camp site to avoid local contamination (mainly exhaust
162 from snow vehicles). Aerosol number concentrations were recorded with resolution of

every 23–25 s (corresponding to 1 liter air sucking) during direct aerosol sampling. The ambient number concentrations were converted to concentration under standard conditions (0 °C and 1013.25 hPa).

2-3-2 Direct aerosol sampling and analysis

Aerosol particles were collected on carbon-coated collodion thin film supported by Ni-microgrid (square-300 mesh; Veco Co.) using a two-stage aerosol impactor. The cut-off diameters of the impactor were 2.0 and 0.2 μm in aerodynamic diameter at a flow rate of 1 liter min^{-1}. The aerodynamic diameter was estimated for particles density of 1 g cm^{-3}. The aerool particle density, however, is mostly larger than 1 g cm^{-3}, for instance, NaCl (2.2 g cm^{-3}), and H_2SO_4 (1.84 g cm^{-3}). Therefore, aerosol particles slightly smaller than the cut-off diameter (aerodynamic diameter) can be collected on the sample substrates, depending on the particle density. The impactor was set at ca. 1 m above the snow surface next the OPC. Because of the lower aerosol number concentrations on the Antarctic continent, direct aerosol sampling was conducted for 28–86 min (mean, 60 min) depending on the aerosol number concentration. After direct sampling, aerosol samples were kept in air tight boxes including desiccant until analysis in our laboratory in Japan to avoid humidification that can engender morphological change, modification (chemical reactions), and fractionation, as described by Hara et al. (2002, 2005, 2013). Therefore, aerosol modification and fractionation might be negligible, although aerosol

183 constituents can be localized in each aerosol particle because of deliquescence of
184 deliquescent aerosol particles under dry conditions.
185
186 Individual aerosol particles on the sample substrate were observed and analyzed in this
187 study using a scanning electron microscope equipped with an energy dispersive X-ray
188 spectrometer (SEM-EDX; Quanta FEG-200F, FEI; XL30; EDAX Inc.). Analytical
189 conditions were the following: 20 kV accelerating voltage and 30 s counting time. To
190 avoid analytical bias of localization of aerosol constituents in each particle, the
191 rectangular or square area almost covering a particle was scanned using an electron
192 beam in EDX analysis. The analytical depth in SEM-EDX analysis depends on the
193 accelerating voltage, chemical composition, density, and other factors. Although
194 secondary electrons can be emitted from a depth of several ~ 10 nm (e.g., Ding et al.,
195 2009), characteristic X-rays can be emitted from a depth of a few μm (e.g., Goldstein *et*
196 *al*. 2007). Most of the coarse particles examined in this study were smaller than 3 μm in
197 diameter. Consequently, characteristic X-rays were obtained from whole particle in fine
198 and coarse mode in this study. When the particle thickness is larger than ca. 5 μm,
199 compositions near surface (thickness of a few micrometers) might be detected. However,
200 only a few particles larger than 5 μm were found in a single sample. Details of
201 analytical procedures and data quality were described by Hara et al. (2002, 2005, 2013).
202 We analyzed 2690 particles in coarse mode (mean: 58 particles / sample) and 45,044

particles in fine mode (mean: 961 particles / sample). Most aerosol-sampled areas on the substrates were analyzed in coarse mode in this study. Although we attempted to analyze as many coarse particles as possible, the lower aerosol number concentrations in coarse mode limit the number of the analyzed aerosol particles in this study. However, 20–30% of the aerosol-sampled area on the substrates was analyzed in aerosol samples in fine mode.

3 Results and Discussion

3-1 Meteorological conditions during the JASE campaign

3-1-2 Air temperature, wind speed, and weather near the surface

Figure 2 shows variations of latitude, elevation, air temperature, and wind speed during the JASE traverse of the Japanese team. The air temperature decreased gradually with latitude in 69−73 °S in both the incoming and outgoing traverse, although the highest temperature near the coast was ca. -7.6 °C in the incoming traverse and -2.9 °C in the outgoing traverse. By contrast, the air temperature was around -30 °C at latitudes higher than 73 °S in this study. The lowest air temperature was -43 °C. In addition, air temperature showed strong diurnal variation. The diurnal temperature range was approximately 8.6 °C on average (maximum, 16 °C).

223 Wind speed often showed diurnal features during the traverse. In addition to diurnal
224 features of wind speed, the wind speed increased because of an approaching cyclone,
225 for example on 18−22 November, 27−30 November, 7–8 December, and 20−23
226 December. Although the diurnal maximum of air temperature was observed at noon
227 time (LT), those of wind speed were lagged at latitudes lower than 73 °S. Similarly,
228 similar diurnal variations of wind speed were observed on Antarctic continent (Allison,
229 1998; Van As et al., 2005) and Antarctic coasts (Sato and Hirasawa, 2007). However,
230 the diurnal maxima of wind speed were mutually synchronized well to those of air
231 temperature at latitudes higher than 74 °S, when their diurnal features occur. According
232 to a manual weather check at every camp site, the weather was mostly clear and fine.
233 When the wind speed was greater than ca. 6 m s^{-1}, drifting snow prevailed during the
234 traverse, for example on 28–29 November, 7 December, and 21–23 December.
235

236 **3-1-2 Air mass history during the JASE traverse**

237 To elucidate the history and origins of air masses observed in this study, the 5-day
238 backward trajectory was computed using the NCEP reanalysis dataset and vertical
239 motion mode in this study (Draxler and Rolph, 2013). Uncertainty of the trajectory
240 analysis derives from the resolution of meteorological data (wind field), calculation
241 scheme, and trajectory model. Kahl et al. (1989) and Stohl et al. (1995) reported that
242 error reached hundreds ~1000 km after trajectory calculation for 5 days. Therefore, the

243 5-day backward trajectory was analyzed in this study. Indeed, previous works (Reijmer
244 et al., 2001, 2002; Hara et al., 2004, 2013; Suzuki et al., 2008) used 5-day backward
245 trajectory analysis to elucidate the origins of moisture and aerosols. In general,
246 uncertainty can be greater when the starting altitude of trajectories is within in boundary
247 layer. The 5-day backward trajectories from altitudes in the boundary layer – free
248 troposphere, however, were closely consistent well with vertical profiles of aerosol
249 constituents over Syowa Station, Antarctica (Hara et al., 2013). For the present study,
250 we calculated the trajectories from 200, 500, and 1000 m above ground level. The
251 trajectories showed similar vertical features and transport pathways in most cases, so
252 that a 5-day backward trajectory might be applied to discuss air mass history even in the
253 Antarctic continent.
254
255 Figure 3 depicts backward trajectories from 200 m above ground level over each camp
256 site. As depicted in Fig. 3a, air masses from the camp sites located in 69–71 °S in the
257 incoming traverse were transported westward along with Antarctic coastal line during
258 the prior 5 days. Vertical features of the backward trajectories imply that these air
259 masses traveled in the upper boundary and lower free troposphere. In contrast to the
260 transport pathway in 69–71 °S, air masses at the camp sites in >71 °S traveled in the
261 free troposphere over the Antarctic continent during the prior 5 days. Air masses in the
262 traverse from Dome F to the meeting point flowed over the Antarctic plateau during the

prior 5 days (Fig. 3b). The vertical motions in these air masses were classified into (1) transport from the free troposphere and (2) travel in the boundary layer (near surface). Compared to the weather at camp sites, the first type (transport from free troposphere) and second type (transport in the boundary layer) respectively corresponded to days with good weather, and to days with strong winds and drifting snow conditions. Backward trajectories in the outgoing traverse from the meeting point to Dome F indicate transport in the boundary layer – lower free troposphere over the Antarctic continent (Fig. 3c). The transport pathway during the outgoing traverse from Dome F to S16 was clearly divisible into transport from coastal areas and transport over the continent (Fig. 3c). Although air masses at latitudes higher than 73 °S traveled over the continent, air masses at >75 °S and at 73–75 °S were transported from near the South Pole, and were transported respectively along ice ridges through near Dome A and Dome C in East Antarctica. Furthermore, air masses in the outgoing traverse moved near ground level (probably in the boundary layer) for the past 5 days, in contrast to the large variation of vertical motions in the incoming traverse from S16 to Dome F. These features of transport pathways of air masses on the Antarctic continent during the JASE traverse showed good agreement with seasonal variations of the air mass origins and transport pathway over the Antarctic continent by Suzuki et al. (2013).

3-2 Number concentrations, mass concentrations, and size distribution of

aerosol particles during the JASE traverse

Figures 4 and 5 depict features of wind speed, the aerosol number concentrations, Junge slope, and aerosol mass concentrations during direct aerosol sampling at each camp site during the JASE traverse. During the incoming traverse, the aerosol number concentrations decreased gradually with latitude and elevation, except high number concentrations in strong winds. Higher aerosol number concentrations were identified under conditions with wind speeds higher than 6 m s^{-1} in this study. Therefore, we use aerosol concentrations at wind speeds lower than 6 m s^{-1} as "background aerosol concentrations" in this study. For instance, the background number concentrations in D_p >0.3 μm and D_p >2 μm changed, respectively, from ca. 1330 L^{-1} near the coast to ca. 160 L^{-1}, and from 36 L^{-1} to 0.5 L^{-1}. The number concentrations on the Antarctic continent during the JASE traverse were lower than those in the lower free troposphere over Syowa Station in summer (Hara et al., 2011b). The aerosol number concentrations increased considerably under strong wind and drifting snow conditions. Considering that air masses on the Antarctic continent during JASE were not transported from coastal areas during the prior 5 days, this increase suggests that strong winds engender the release of aerosol particles and small snow/ice flakes from the snow surface. Particularly the number concentrations in coarse particles having diameter larger than 2.0 μm increased remarkably by 1–2 orders higher in strong wind conditions, as shown in Figs. 4 and 5. The aerosol number concentrations and their horizontal features in the

303 outgoing traverse were similar to those in the incoming traverse.

304

305 For comparison of the aerosol size distribution, we estimated the "Junge-slope" in this
306 study. The aerosol size distribution in fine–coarse mode can be approximated as the
307 following equation (Junge, 1963).

308

309 $$\frac{dN}{d\log D_p} = \alpha D_p^{-\beta}$$

310

311 Therein, α and β respectively represent a constant and the Junge-slope. The Junge slope
312 is often used as an index of the shape of aerosol size distribution in fine–coarse modes.
313 For instance, higher (lower) Junge-slope values are visible, respectively, in cases of high
314 (low) number concentrations in fine mode and/or low (high) concentrations in coarse
315 mode, respectively. In this study, the Junge slope (β) was estimated as 0.3–5.0 μm in
316 diameter. The Junge slope was 2.22–3.03 (mean, 2.70; median, 2.75) in background
317 conditions (wind speed lower than 6 m s^{-1}) in the incoming traverse. In contrast, the
318 Junge slope decreased to less than 2.5 under conditions with strong winds (>6 m s^{-1}) or
319 drifting snow. The Junge slope in the outgoing traverse was 2.73–3.37 (mean, 3.03;
320 median, 2.92) under background conditions. Similar to the Junge slope in the incoming
321 traverse, the Junge slope decreased in strong winds during the outgoing traverse. The

322 considerable decrease of June slope in strong wind corresponded to high number
323 concentrations in coarse mode (Figs. 4-5). Consequently, aerosol size distributions
324 depended closely on release of aerosol particles from snow surfaces by blowing winds.
325 In addition, the Junge slopes in the outgoing traverse were slightly larger than those in
326 the incoming traverse. This difference derived from the reduction of aerosol release
327 (especially in coarse mode) from the snow surface under calm wind conditions during
328 the outgoing traverse. Considering that weather conditions are usually stable in
329 December–January on the Antarctic region (e.g., Sato and Hirasawa, 2007), these
330 differences between the incoming traverse and outgoing traverse might reflect seasonal
331 features of aerosol number concentrations and the size distribution on the Antarctic
332 continent during early summer (or end-spring) through mid-summer. Compared to the
333 Junge slope in the lower troposphere over Syowa Station during the summer (range,
334 2.2–3.2; median, 2.5; Hara et al., 2011b), the Junge slope was slightly greater on the
335 Antarctic continent during the JASE traverse. The difference of the Junge slopes might
336 result from horizontal features of the number concentrations, particularly in coarse
337 mode, from coasts to inland areas. Indeed, the number concentrations in coarse mode in
338 JASE traverse were several factors – one order lower than those over Syowa Station.
339
340 Here, we attempt to estimate the mass concentrations using aerosol number
341 concentrations measured with OPC. The spherical shape and density were assumed in

342 the estimation. As described above, diameters in OPC are the "optically PSL-equivalent
343 size", so that the estimated aerosol volume means "PSL-equivalent volume" in this
344 study. The densities corresponded to those of sulfates (ca. 1.8 g cm^{-3}) and NaCl (2.2 g
345 cm^{-3}). Major aerosol constituents were sulfate particles during JASE traverse (details are
346 presented later herein). Therefore, we used the density of 1.8 g cm^{-3} to estimate the mass
347 concentration in this study. The number concentrations of aerosol particles smaller than
348 0.3 μm were not included in the estimation. Therefore, the estimated mass
349 concentrations can be slightly underestimated. In addition, the aerosol number
350 concentrations were observed using OPC above the snow surface. Consequently, the
351 number concentrations were measured under ambient conditions (not dry conditions),
352 although OPC had been packed in an insulator box. Therefore, the estimated mass
353 concentrations included masses of water in aerosol particles in this study. The presence
354 of water in aerosol particles can cause overestimation of the aerosol density and mass
355 concentrations because of salt dilution by water.
356
357 With the exception of higher mass concentrations under conditions with drifting snow
358 and strong winds, the aerosol mass concentrations decreased gradually from ca. 0.16 μg
359 m^{-3} (near the coasts) to 0.04 μg m^{-3} (near Dome F Station). The mass concentrations on
360 the Antarctic continent during JASE traverse were similar to the mass concentrations of
361 water soluble aerosol constituents at Kohnen Station (Weller and Wagenbach, 2007).

362 They were slightly higher than the mass concentrations water soluble aerosol
363 constituents at Dome C (Preunkert et al., 2008; Udisti et al., 2010). The aerosol mass
364 concentrations increased considerably to greater than several milligrams per cubic meter
365 under conditions with drifting snow and strong winds. The highest mass concentrations
366 were approximately 5.7 μg m^{-3}. Higher mass concentrations were observed in high
367 number concentrations in coarse mode. Therefore, aerosol particles from the snow
368 surface by erosion under strong winds might make a substantial contribution to high
369 aerosol mass concentrations.
370
371 Figure 3 shows that air masses on the Antarctic continent were transported over the
372 Antarctic plateau during the prior 5 days. Considering that coarse particles can be
373 removed efficiently from the atmosphere through dry deposition during transport,
374 isolation from coastal regions might account for gradient features of aerosol number
375 concentrations in coarse mode. In other words, coarse particles are supplied only
376 slightly from coastal regions into the Antarctic plateau during summer. The aerosol
377 number concentrations increased markedly in all size ranges (D_p >0.3 μm) under strong
378 wind conditions. Therefore, the wind-blowing release of aerosol particles might play an
379 important role in maintaining the aerosol system over the continent in addition to gas-
380 to-particle conversion.
381

382 ### 3-3 Morphology of aerosol particles collected during the JASE traverse

383 Figure 6 depicts examples of SEM images of aerosol particles collected during the
384 JASE traverse. Figure 6a shows that most aerosol particles in fine mode had a satellite
385 structure. The satellite particles were dominant in all samples in fine mode (D_p: 0.2–2
386 μm). The satellite particles were often observed also in coarse mode (D_p > 2 μm) in this
387 study. Yamato et al. (1987) used chemical tests (Ca thin film method) to show that
388 satellite particles consisted of H_2SO_4 in the Antarctic troposphere during summer. Figure
389 6b shows that aerosol particles without a satellite structure were also observed in coarse
390 mode. Most non-satellite particles in coarse mode had a solid core with irregular shape
391 and crystal-like shape. In addition, stain around the solid core was identified often in
392 coarse mode, as depicted in Fig. 6b. Some coarse particles were satellite particles with
393 irregular solid cores (not shown). Presence of the stain and satellite structure in coarse
394 and fine modes suggests strongly that these particles had liquid phase in the atmosphere.
395

396 ### 3-4 Aerosol constituents and mixing states during the JASE traverse

397 Figure 7 presents examples of EDX spectra of each aerosol particle collected during the
398 JASE traverse. Although strong peaks of C, O, and Ni were detected in all samples,
399 these peaks were derived from the sample substrate. Therefore, C, O, and Ni were
400 excluded from discussion in this study. As portrayed in Fig. 7a, strong peaks of S were
401 observed from aerosol particles with a satellite structure. Comparison among the

402 elemental compositions, morphology (satellite structure), and previous investigations by
403 Yamato et al. (1987) and Hara et al. (2013) showed that these particles might consist
404 mainly of H_2SO_4 and CH_3SO_3H, which are derived mainly from oceanic bio-activity.
405 Because EDX can provide only elemental information, we cannot distinguish SO_4^{2-}
406 from $CH_3SO_3^-$. Hereinafter, we designate these aerosol particles as "sulfate particles".
407
408 In fact, S and K were detected from aerosol particles as shown in Fig. 7b. Aerosol
409 particles containing S and K had no satellite structure. Similar aerosol particles were
410 identified in aerosol samples taken in the lower free troposphere – upper free
411 troposphere in Antarctic region (Hara et al., 2010, 2013).
412
413 Peaks of Mg and S were obtained from aerosol particles as portrayed in Fig. 7c. Atomic
414 ratios of Mg and S of the aerosol particles containing only Mg and S were compatible
415 with the ratios of $MgSO_4$. Mg-rich sulfate particles in the lower troposphere over Syowa
416 Station were identified dominantly in air masses transported from the Antarctic
417 continent (Hara et al., 2013). Hara et al. (2013) reported that Mg-rich sulfate particles in
418 the Antarctic atmosphere were associated with sea-salt fractionation and sea-salt
419 modification. Details of Mg-rich sulfate particles and sea-salt fractionation are
420 discussed in section 3-7.
421

Aerosol particles containing Ca and S were also observed in this study (Fig. 7d). Because of the atomic ratios of Ca and S, particles of this type might be $CaSO_4$ particles. $CaSO_4$ particles were identified in the lower troposphere on the Antarctic region (Hara et al., 2010, 2013). Actually, $CaSO_4$ is well known as a major mineral constituent (gypsum). Moreover, Marion and Farren (1999) and Geilfus et al. (2013) pointed out $CaSO_4$ (gypsum) formation by sea-salt fractionation on sea ice in polar regions. However, the origins of $CaSO_4$ particles in the Antarctic atmosphere remain unclear.

Peaks of Na, Mg, S, and Cl were obtained in aerosol particles as shown in Fig. 7e. These elements are major seawater constituents. When artificial NaCl particles were analyzed using SEM-EDX, the peak height of Cl was slightly higher than that of Na.

Consequently, the particle in Fig. 7e might be identified as partly Cl-depleted sea-salt particles. In addition, Na, Mg, and S were detected from the aerosol particle in Fig. 7f. Compared to the aerosol particle in Fig. 7e, the peak height of S relative to Na was higher in the particle in Fig. 7f. Additionally, the height of Mg relative to Na was higher than that of sea-salt particles depicted in Fig. 7d. The particle in Fig. 7f might be identified as a wholly Cl-depleted sea-salt particle with slight Mg-enrichment. Although Na, Mg, and S were detected from the aerosol particle in Fig. 7g, the peak height of S was lower than the particles in Figs. 7e-7f. In addition, the particle in Fig. 7g might be

identified as a wholly Cl-depleted sea-salt particle. Hereinafter, we designate wholly Cl-depleted particles as “modified sea-salt particles”. Less Cl-depleted sea-salt particles and partially Cl-depleted sea-salt particles were divided into “sea-salt particles” in this study. Modification of sea-salt particles is discussed in section 3-6. Although Mg is a major sea-salt constituent, Mg was not detected from aerosol particles containing Na, K, and Cl, as portrayed in Fig. 7h. A particularly strong K peak relative to Na peak was identified clearly from the particle in Fig. 7h. Na is a dominant constituent in sea-salt particles. Therefore, particles of this type were identified as “sea-salt-like particles” in this study. The sea-salt-like particles were observed only at sampling sites on the way from Dome F to the meeting point in the incoming traverse on 21–23 December, 2007 when aerosol particles were collected under conditions with drifting snow.

In fact, Si, Al, and S were detected from solid particles as shown in Fig. 7i. Results show that Al and Si were major constituents. Therefore, particles of this type might be identified as mineral particles. Here, aerosol particles containing Si and Al were classified into “mineral particles”. Furthermore, stain and satellite structures were observed around irregular solid core in some mineral particles. Considering that S was detected in mineral particles (irregular solid particles) satellite structure, these particles were likely to be mineral particle coated by acidic sulfates and H_2SO_4. In addition, internal mixtures of minerals and sea-salt particles were often identified in this study

(Fig. 7j).

3-5 Horizontal distributions of aerosol constituents during the JASE traverse

To compare quantitatively horizontal distributions of each aerosol constituent and mixing states, we estimated the relative abundance (number fraction) of each type of aerosol constituent. Considering the mean analyzed particles in each sample, the detection limit of relative abundance was ca. 0.1% in fine mode and 1-2% in coarse mode except for samples with lower aerosol density on the substrate in coarse mode. Figures 8 and 9 show horizontal distributions of relative abundance of aerosol mixing states in coarse and fine modes during the incoming traverse (14 November – 27 December 2007) and the outgoing traverse (27 December 2007 – 24 January 2008).

3-5-1 Sea-salts

In coarse mode, major aerosol particles were sea-salt particles, modified sea-salt particles and sulfate particles. The relative abundance of sea-salt particles in coarse mode was larger than 40% near the coast in the incoming traverse. Relative abundance of sea-salt particles in coarse mode decreased gradually in inland areas, with exception of the high abundance at sampling sites in 77–76 °S on the way from Dome F Station to the meeting point in the incoming traverse (Fig.8d). As described above, sea-salt-like

particles (Na–K–Cl) were observed predominantly in coarse mode at these sites. With the gradual decrease of the relative abundance of sea-salt particles, the relative abundance of the modified sea-salt particles increased gradually up to 40% on the Antarctic plateau. By contrast, the modified sea-salt particles were dominant in fine mode in the incoming traverse. Because of the predominance of sulfate particles in fine mode, the relative abundance of sea-salt particles and the modified sea-salt particles was less than 6.8% even at latitudes lower than 72 °S and less than 2.8% at latitudes higher than 72 °S during the incoming traverse. According to the 5-day backward trajectory as depicted in Fig. 3, transport from the coasts was found only at 69–71 °S during the incoming traverse, whereas air masses in the inland area (>72 °S) were transported over the continent during the prior 5 days. Therefore, isolation from the coastal regions might cause gradual distributions of sea-salt particles and modified sea-salt particles in the continent. The transport pathway, however, cannot account for the high relative abundance of sea-salt particles and the modified sea-salt particles, for example at 72–73 °S and at 77–76 °S. As depicted in Fig. 4, the aerosol number concentrations increased considerably, particularly in coarse mode, under strong wind conditions in the incoming traverse to the meeting point. Consequently, high aerosol number concentrations and their high relative abundance might result from redistribution of aerosol particles such as sea-salt particles from the snow surface. Therefore, the horizontal distribution of relative abundance of sea-salt particles and the modified sea-salt particles on the

502 Antarctic continent during summer might be associated with the transport pathway and
503 release from the snow surface via wind-blowing.
504
505 Relative abundance of sea-salt particles and the modified sea-salt particles in coarse
506 mode ranged mostly lower than 60% during the outgoing traverse. Although the total
507 relative abundance of sea-salt particles and the modified sea-salt particles in coarse
508 mode was similar to that in the incoming traverse except for the high relative abundance
509 under strong wind conditions, the modified sea-salt particles were dominant in the
510 outgoing traverse. However, the relative abundance of sea-salt particles and the
511 modified sea-salt particles in fine mode was mostly less than 0.5% in inland areas
512 during the outgoing traverse. In some samples taken on the Antarctic plateau, sea-salt
513 particles and the modified sea-salt particles were not detected in fine mode. Compared
514 to the horizontal distributions of sea-salt particles and the modified sea-salt particles in
515 fine mode during the incoming traverse, relative abundances of sea-salt particles and the
516 modified sea-salt particles were remarkably lower. Mass concentrations of sea-salts
517 (Na^+) in aerosol particles show a minimum at Syowa and Dome F stations during
518 summer (Hara et al., 2004). In addition, the relative abundance of sea-salt particles and
519 the modified sea-salt particles decreased considerably over Syowa Station (Hara et al.,
520 2013). Although blizzard attributable to approaching cyclone occurs until early
521 December at Syowa Station, few blizzards occur usually in mid-December – January

(Sato and Hirasawa, 2007). The seasonal feature of approaching cyclone are closely related to the origins of air masses over the Antarctic continent, as suggested by Suzuki et al. (2013). Therefore, the difference of the relative abundance between in the incoming traverse and in the outgoing traverse might correspond to seasonal features of sea-salt particles, air mass origins, and transport pathway from the end of spring to summer on the Antarctic continent.

3-5-2 Sulfates

As classified in section 3-4, the following aerosol particles containing sulfates were identified in this study: (1) sulfate particles, (2) modified sea-salt particles, (3) sulfate particles containing K, (4) $MgSO_4$ particles, (5) $CaSO_4$ particles, and (6) mineral particles internally mixed with sulfates. Because horizontal distributions of the modified sea-salt particles and mineral particles are internally mixed with sulfates were described, respectively, in sections 3-5-1 and 3-5-3, their description is excluded from this section.

Figures 8 and 9 show that sulfate particles were the major aerosol particles in coarse mode and that they were dominant in fine modes. Particularly, the mean relative abundance of sulfate particles in fine mode was 98.5% in the incoming traverse and 99.5% in the outgoing traverse. In some samples taken on the Antarctic plateau, the relative abundance of sulfate particles in fine mode reached 100% in incoming and

outgoing traverses. Considering detection limits of the relative abundance in fine mode, the upper limit of relative abundance of aerosol particles other than sulfate particles might be less than 0.1% in these samples (100% abundance of sulfate particles). Higher relative abundance of sulfate particles in the outgoing traverse is likely to result from (1) increase of the number concentrations of sulfate particles in fine mode by particle growth of ultrafine sulfate particles by hygroscopicity, (2) cloud processes, and (3) decrease of the number concentration of sea-salt particles and the modified sea-salt particles during the summer. Indeed, mass concentrations of nss-SO_4^{2-} and sea-salts (Na^+), respectively showed a maximum and minimum in the summer (January–February) along the Antarctic coast and inland (e.g., Minikin et al., 1998; Hara et al., 2004; Weller and Wagenbach, 2007; Preunkert et al., 2008; Udisti et al., 2012). The relative abundance of sulfate particles in fine mode was 82.9–98.2% (mean, 93.1%) in the boundary layer and 96.2–99.7% (mean, 98.1%) in the lower free troposphere over Syowa Station, Antarctica during mid-November through January (Hara et al., 2013). Consequently, the relative abundance of sulfate particles in fine mode near the surface on the Antarctic continent was similar to that in the lower free troposphere over the Antarctic coast (Syowa Station). The relative abundance of sulfate particles in coarse mode often exceeded 40% on the Antarctic continent during the JASE traverse. Such a high relative abundance of coarse sulfate particles was not observed in the boundary layer but often in the lower free troposphere over Syowa Station (Hara et al., 2013). As

described above, "sulfate particles" in this study did not contain Na, Al, and Si. Therefore, these particles might be composed of SO_4^{2-} and $CH_3SO_3^-$ as suggested by Hara et al. (2005). In addition, chemical tests using Ca thin film method implied that aerosol particles containing SO_4^{2-} were present as acidic states (i.e., sulfuric acid particles) (Yamato et al., 1987a, 1987b). Consequently, sulfate particles might be grown to coarse mode through (1) hygroscopic growth, (2) cloud processes, (3) heterogeneous sulfate formation and (4) coagulation and condensation of condensable vapors (e.g., H_2SO_4 gas) under conditions with low number concentrations of pre-existing particles on the Antarctic continent.

The relative abundance of K-rich sulfate particles was not detected (n.d.) – 2.0% in coarse mode and n.d. – 0.9% in fine mode in this study. Although K-rich sulfate particles were obtained in a few samples in coarse mode, these particles were observed often in fine mode in this study. Moreover, K-rich sulfate particles were often observed in the incoming traverse. In addition, the relative abundance of K-rich sulfate particles in the incoming traverse was higher than that in the outgoing traverse. K-rich sulfate particles were distributed also in boundary layer – upper free troposphere over Syowa Station (Hara et al., 2010, 2013). Actually, K-rich sulfate particles cannot be formed through gas-to-particle conversion from aerosol precursors derived from oceanic bioactivity. Therefore, K-rich sulfate particles might be non-biogenic aerosol particles.

As discussed by Okada et al. (2001, 2008) and Niemi et al. (2005), K-rich sulfate particles and nss-K in aerosol particles are released from combustion processes such as biomass burning.

As discussed above and by Hara et al. (2013), K-rich sulfate particles might have originated from biomass burning and fossil fuel combustion. As shown in Figure 3, direct transport from outsides of the Antarctic Circle was not found for the prior 5 days. Moreover, the source strength of combustion of fossil fuel is extremely low in Antarctic regions. Particularly, biomass burning does not occur in the Antarctic regions. Therefore, sulfate particles containing K were likely to have been transported to the Antarctic continent via the free troposphere during summer for the prior 5 days. The presence of combustion-origin aerosol particles (e.g., sulfate particles containing K) was supported by high BC concentrations at the South Pole in the summer (Bodhaine, 1995). This difference of relative abundance in incoming and outgoing traverses might be attributed to seasonal features of K-rich sulfate particles, air mass origins, and transport pathway in the inland area during late spring – summer.

The relative abundance of Mg-rich sulfate particles (probably $MgSO_4$) examined in this study was n.d. – 1.8% in coarse mode and n.d.–0.5% in fine mode. During the incoming traverse, Mg-rich sulfate particles were found frequently in fine mode at sampling sites

602 in 69.2–72.5 °S, although those were observed in some aerosol samples collected at
603 plateau sites. However, Mg-rich sulfate particles were identified mainly on the Antarctic
604 plateau during the outgoing traverse. The relative abundance of Mg-rich sulfate particles
605 was lower in the outgoing traverse than that in the incoming traverse. Mg-rich sulfate
606 particles were distributed mostly in fine mode over Syowa Station (Hara et al., 2013).
607 An earlier investigation (Hara et al., 2013) showed that Mg-rich sulfate particles were
608 associated with sea-salt fractionation (Mg separation) and modification (Cl loss by
609 heterogeneous reactions). Consequently, the presence of Mg-rich sulfate particles in the
610 atmosphere near the surface on the Antarctic continent in this study strongly suggests
611 that sea-salt fractionation occurs on the Antarctic continent during summer. Details of
612 sea-salt fractionation are discussed in section 3-7.
613
614 Relative abundance of Ca-rich sulfate particles (probably $CaSO_4$) was n.d. – 8.7% in
615 coarse mode and n.d. – 0.2% in fine mode in the incoming traverse. However, the
616 relative abundance of Ca-rich sulfate particles was n.d. in coarse mode and n.d. – 0.1%
617 in the outgoing traverse. Although Ca-rich sulfate particles were not detected in most
618 samples in either traverses, Ca-rich sulfate particles were identified mainly near coasts
619 (<72°S). Although Ca-rich sulfates such as gypsum are mineral components, most Ca-
620 rich sulfates were not mixed with Al and Si, which are major elements of mineral
621 particles. Consequently, horizontal distributions and external mixing states of Ca-rich

622 sulfates imply the important contribution of non-mineral origins such as sea-salt
623 fractionation on sea ice as reported by Geilfus et al. (2013).
624
625 **3-5-3 Minerals**
626 The relative abundance of mineral particles ranged in n.d. – 14.6% in coarse mode and
627 n.d. – 0.4% in fine mode during the incoming traverse, although the relative abundance
628 ranged in n.d. – 5.7% in coarse mode and n.d. – 0.1% in fine mode during the outgoing
629 traverse. Mean relative abundance in coarse mode was 3.8 and 1.8 % in incoming and
630 outgoing traverses, respectively, and that in fine mode was 0.1 % and 0.01 % in
631 incoming and outgoing traverses. Most mineral particles were internally mixed with
632 sea-salts or sulfates in this study. Although the mineral particles were observed mainly
633 in coarse mode, SEM-EDX analysis showed that the size of irregular solid cores
634 containing Al and Si was of sub-micrometer in this study. The size of irregular solid
635 cores was coincident with the size distribution of water-insoluble particles (mainly
636 mineral particles) in ice cores taken in Antarctica (e.g., Ram and Gayley, 1988;
637 Delmonte et al., 2004, 2007). In contrast, external mixing states of mineral particles
638 were often present in the boundary layer and free troposphere over Syowa Station
639 located at the coast (Hara et al., 2006, 2013). The difference of mixing states of mineral
640 particles suggests that mixing states of mineral particles changed gradually to internal
641 mixtures through coagulation in cloud processes, and through heterogeneous reactions

642 during their transport to inland areas. As described above, a change of mixing state of
643 mineral particles can engender particle sizes greater than the external mixing states of
644 mineral particles. Because of the higher dry deposition velocity of coarse aerosol
645 particles, internal mixing among minerals, sulfate, and sea-salts during transport might
646 enhance the efficient deposition of minerals onto the snow surface on the Antarctic
647 continent.
648
649 **3-6 Sea-salt modification during the JASE traverse**
650 **3-6-1. Sea-salt modification in coarse and fine modes**
651 Figure 10 portrays examples of ternary plots (Na–S–Cl) of sea-salt particles and the
652 modified sea-salt particles during the JASE traverse. To avoid misunderstanding of sea-
653 salt modification, the internal mixed sea-salt and mineral particles were excluded from
654 the ternary plots and discussion. Red and blue stars respectively denote atomic ratios of
655 bulk seawater ratios and wholly Cl depleted sea-salt particles by SO_4^{2-}. The black line
656 represents the stoichiometric line from the sea salt particles with bulk seawater ratio
657 (red star) to the Cl-depleted sea salt particles by sulfates (blue star). When Cl in sea-salt
658 particles is replaced stoichiometrically to SO_4^{2-} by heterogeneous reactions, each sea
659 salt particle is distributed along the stoichiometric line.
660
661 Most sea-salt particles in coarse mode had Cl ratios lower than the seawater ratio in this

662 study. Although S ratios increased gradually with decreased Cl ratios in sea-salt
663 particles, the S ratios in sea-salt particles were less than those of the stoichiometric line
664 on the Antarctic continent during summer, which suggests that sea-salt particles were
665 modified not only with SO_4^{2-} but also with acidic species other than acidic sulfur
666 species such as SO_4^{2-}. Plausible acidic species other than SO_4^{2-} and $CH_3SO_3^-$ for Cl loss
667 from sea-salt particles are reactive nitrogen oxides such as HNO_3, N_2O_5, and NO_3 (e.g..,
668 Hara et al., 1999) and organic acids (Kerminen et al., 2000; Laskin et al., 2012).
669 Previous studies of aerosol chemistry in Antarctic regions showed that NO_3^-
670 concentrations were higher than those of organic acids (oxalate, formate, and acetate)
671 (Jourdain and Legrand, 2002; Weller et al., 2002, 2007; Rankin and Wolff, 2003;
672 Legrand et al., 2004; Hara et al., 2010; Weller et al., 2011). Furthermore, higher
673 concentrations of reactive nitrogen oxides (e.g., HNO_3 and NO) were observed on the
674 Antarctic continent and coasts during summer (Davis et al., 2004; Dibb et al., 2004;
675 Jones et al., 2011). Details of origins of the reactive nitrogen oxides are discussed in the
676 next section. Therefore, heterogeneous NO_3^- formation on sea-salt particles might make
677 an important contribution to sea-salt modification in inland areas during summer. In
678 contrast to sea-salt modification in coarse mode, most of the modified sea-salt particles
679 in fine mode were distributed in the Cl ratio of ca. 0% and higher S atomic ratio relative
680 to the modified sea-salt particles. Therefore, fine sea-salt particles on the Antarctic
681 continent might be modified preferentially with acidic sulfur species such as SO_4^{2-} and

682 $CH_3SO_3^-$.

683

684 **3-6-2. Horizontal features of sea-salt modification on the Antarctic**
685 **continent**

686 Figures 11 and 12 respectively portray horizontal features of the atomic ratios of Cl/Na
687 and S/Na of sea-salt particles and the modified sea-salt particles in coarse and fine
688 modes during the incoming and outgoing traverses. The internal mixing particles
689 between sea-salts and minerals were excluded from the box plots. A latitudinal gradient
690 of Cl/Na ratios in coarse mode was observed in 69–71 °S in the incoming traverse. High
691 Cl depletion was identified in most aerosol samples obtained for the Antarctic plateau,
692 except for some samples taken at 76.5–76 °S in the incoming traverse from Dome F to
693 the meeting point. In spite of the latitudinal gradient of Cl/Na ratios in coarse mode in
694 69–71 °S in the incoming traverse, the S/Na ratio increased slightly. Similarly, median
695 S/Na ratios of sea-salt particles and the modified sea-salt particles in coarse mode were
696 distributed approximately around 0.2 during the JASE traverse. When sea-salt particles
697 are modified solely with SO_4^{2-}, the S/Na ratios in sea-salt particles are 0.5. As suggested
698 in ternary plots in Fig. 10, therefore, NO_3^- contributed dominantly to sea-salt
699 modification in coarse mode on the Antarctic continent.

700

701 Hara et al. (2005, 2013) reported that most sea-salt particles in coarse mode were

modified slightly over Syowa station in the summer. Some were modified with SO_4^{2-}. Consequently, the acids contributing to sea-salt modification differed between those in coarse sea-salt particles on the Antarctic coasts and those on the continent during summer. The air mass history and origins of coarse sea-salt particles, NO_3^-, and its precursors on the Antarctic continent must be discussed to elucidate the strong contribution of NO_3^- to sea-salt modification. The 5-day backward trajectory, as depicted in Fig. 3, shows that continental air masses on the Antarctic plateau had not been transported directly from coasts during the prior 5 days. Because of efficient dry deposition of coarse aerosol particles, coarse particles suspended at the Antarctic coasts might be transported only slightly to the Antarctic continent (particularly the Antarctic plateau) for longer than 5 days. As discussed in sections of 3-2 and 3-5-1, most coarse sea-salt particles on the Antarctic plateau were likely to have originated from surface snow on the Antarctic continent. Figures 11 and 12 show that high Cl/Na ratios on the Antarctic plateau often corresponded to conditions with strong winds and drifting snow. Consequently, sea-salt particles might have high Cl/Na ratios immediately after release from the snow surface. Then, sea-salt particles in coarse mode might be modified gradually with reactive nitrogen oxides such as HNO_3 in the continental atmosphere during transport over the Antarctic continent.

Field measurements of the surface snow in polar regions (e.g., Davis et al., 2001, 2004;

722 Frey et al., 2009; Jones et al., 2011) implied photochemical-recycling mechanisms of
723 snow-nitrate near the surface of polar regions during summer. Indeed, high NO
724 concentrations (order of several hundred pptv) were observed at the South Pole Station
725 during summer (Davis et al., 2001; Neff et al., 2008). Actually, NO_x can be converted to
726 HNO_3 in the atmosphere. Therefore, the high NO_x concentration during summer on the
727 Antarctic plateau might engender efficient HNO_3 production near the surface, as
728 suggested by Dibb et al. (2004). Considering the high NO_3^- concentration in the surface
729 snow around Queen Maud Land, especially around Dome F Station (Bertler et al., 2005),
730 considerable HNO_3 production in the atmosphere might occur on the Antarctic plateau.
731 Therefore, sea-salt modification in coarse mode through heterogeneous reactions with
732 reactive nitrogen oxides (mainly HNO_3) might occur preferentially on the Antarctic
733 continent during summer.
734
735 By contrast, S/Na ratios in fine sea-salt particles exceeded mostly 0.5 during the
736 traverse. The high S/Na ratios in each sea-salt particle in fine mode imply that sulfates
737 were formed on the fine sea-salt particles through heterogeneous reactions with gaseous
738 sulfur species such as H_2SO_4 and SO_2. High S/Na ratios in the modified sea-salt
739 particles were also obtained in the boundary layer and lower free troposphere over
740 Syowa Station during summer (Hara et al., 2013). Because of the longer residence time
741 of fine aerosol particles, the modified sea-salt particles in fine mode with high S/Na

742 ratio might be supplied by transport from coastal regions to the continent and might be
743 formed through heterogeneous processes during transport.
744
745 **3-7 Sea-salt fractionations on the Antarctic continent during summer**
746 **3-7-1. Sea-salt fractionations in coarse and fine mode**
747 Figure 13 shows examples of ternary plots of sea-salts (Na, Mg, and S) and Mg-rich
748 sulfates in coarse and fine modes. Internal mixtures of sea salts and minerals were
749 removed from the ternary plots. In the ternary plots, sea-salt particles with bulk
750 seawater ratio are distributed around the red star (bulk seawater ratio). When the sea-salt
751 particles are modified by sulfate and are not fractionated, they are distributed around the
752 stoichiometric line between the red star (seawater ratio) and the blue star (modified sea-
753 salt ratio with sulfate). With sea-salt fractionation by precipitation of Na-salts such as
754 mirabilite (Na_2SO_4 $10H_2O$) and hydrohalite (NaCl $2H_2O$) (Hara et al., 2012), Mg in sea-
755 salt particles can be enriched gradually. For cases in which sea-salt fractionation
756 (replacement between Na and Mg) occurs without sea-salt modification by sulfate, sea-
757 salt particles are distributed around the stoichiometric line between the red star (bulk
758 seawater ratio) and the cyan star ($MgCl_2$). When sea-salt fractionation and sea-salt
759 modification by sulfate occur stoichiometrically and simultaneously, sea-salt particles
760 are distributed around the stoichiometric line between the red star (seawater ratio) and
761 the green star ($MgSO_4$).

762

763 Because sea-salt particles were modified dominantly during JARE (as shown in Figs.
764 10–12), most sea-salt particles and the modified sea-salt particles in coarse mode were
765 distributed in 60–90% of the Na atomic ratio. The Mg ratios in coarse mode, however,
766 were greater than the stoichiometric line of sea-salt modification (between the red star
767 and blue star). Some of the modified sea-salt particles had Mg ratio ≈ 0, even in coarse
768 mode. The Mg ratios in fine mode were distributed at Mg ratio ≈ 0 and around the
769 stoichiometric line between the red star (seawater) and green star ($MgSO_4$). Here, we
770 designate sea-salt particles with Mg ratio ≈ 0 as "Mg-free sea-salt particles". In addition
771 to Mg-free sea-salts, $MgSO_4$ particles were often observed in this study, as shown in
772 Figs. 7–9 and 13. Similar distributions were observed in sea-salt particles and the
773 modified sea-salt particles collected over Syowa Station (Hara et al., 2013). The Mg/Na
774 ratios cannot be changed by sea-salt modification. Sea-salt fractionation in sea ice
775 regions during winter through spring (e.g., precipitation of mirabilite and hydrohalite)
776 can promote Mg enrichment in sea-salt particles, as reported by Hara et al. (2012).
777 Consequently, sea-salt fractionation in sea ice regions cannot account for the presence
778 of Mg-Free sea-salt particles during spring–summer. Because Mg-rich sulfate particles
779 over Syowa Station were identified in the air masses from the Antarctic continent (Hara
780 et al., 2013), discussion must address horizontal features of Mg-rich sulfates, Mg-rich
781 sea-salt particles and Mg-free sea-salt particles on the Antarctic regions. Then it will be

782 possible to assess the possibility of sea-salt fractionation on the Antarctic continent.

783

784 **3-7-2. Horizontal features of sea-salt fractionation on the Antarctic**

785 **continent**

786 To elucidate sea-salt fractionation on the Antarctic continent during summer, we must

787 compare horizontal features of sea-salt constituents on the Antarctic continent. Figures

788 14 depicts horizontal features of Mg/Na ratios in coarse and fine modes during the

789 JASE traverse. Internal mixtures of sea salts and minerals were removed from the plots.

790 Mg/Na ratios in fine mode were varied largely in coming traverse. Because of lower

791 relative abundance of sea-salt particles and the modified sea-salt particles in fine mode,

792 horizontal features of Mg/Na ratios in fine mode were obtained only in 69–73.5 °S in

793 the incoming traverse. The large variation of Mg/Na ratios might be attributed to

794 presence of Mg-rich sea-salt particles and Mg-free sea-salt particles in fine mode, as

795 shown in the ternary plots (Fig. 13). Median Mg/Na ratios in coarse mode were

796 approximately 0.32 in the incoming traverse and 0.31 in the outgoing traverse. Because

797 of Mg/Na ratio ≈ 0.11 in bulk seawater (e.g., Wilson, 1975), Mg might be enriched in

798 most sea-salt particles in coarse mode. In addition, Mg-free sea-salt particles (Mg/Na

799 ratio ≈ 0) in coarse mode were identified often on the Antarctic continent, particularly

800 on the Antarctic plateau. For example, Mg-free sea-salt particles in coarse mode were

801 dominant in three samples taken on 21–23 December, 2007 (76.6–76.0 °S) in the

802 traverse from Dome F to the meeting point, as shown in Fig. 14. The presence of Mg-
803 free sea-salt particles in coarse mode corresponded often to occurrence of drifting snow
804 and high aerosol number concentrations in coarse mode in the incoming traverse. Mg-
805 rich sea-salt particles, Mg-free sea-salt particles, and $MgSO_4$ particles were present also
806 in fine mode on the Antarctic continent, although the low relative abundance of sea-salt
807 particles and the modified sea-salt particles prevented us from elucidating the horizontal
808 features of Mg/Na ratios on the Antarctic plateau. These horizontal features of Mg/Na
809 ratios during the JASE traverse imply strongly that the fractionated sea-salt particles
810 were distributed widely throughout the Antarctic continent during summer. Mg-free sea-
811 salt particles were identified mainly in fine mode and rarely in coarse mode over Syowa
812 Station (Hara et al., 2013). Figure 3 shows that air masses on the Antarctic plateau were
813 isolated from coastal regions for the prior 5 days. The lower relative abundance of Mg-
814 free sea-salt particles in coarse mode over Syowa Station suggests that Mg-free sea-salt
815 particles and other fractionated sea-salt particles such as Mg-rich sulfates and Mg-rich
816 sea-salts had not originated from coastal regions, considering the efficient dry
817 deposition of aerosol particles in coarse mode. Aerosol particles on the Antarctic plateau,
818 especially in coarse mode, were supplied to a marked degree from snow surface by
819 wind blowing under strong conditions, as described above. Furthermore, Mg-rich
820 sulfates and Mg-free NaCl were present in surface snow (Iizuka et al., 2012). Therefore,
821 the fractionated sea-salt particles (Mg-rich sea-salt particles, Mg-free sea-salt particles,

822 and $MgSO_4$ particles) might have originated from surface snow on the Antarctic
823 continent. Considering that Mg-free sea-salt particles were often observed under strong
824 wind conditions (especially on 21–23 December), strong winds might be necessary for
825 the release of Mg-free sea-salt particles.
826
827 To explain the presence of Mg-rich sea-salt particles, Mg-free sea-salt particles and
828 $MgSO_4$ particles on the snow surface of the Antarctic continent, it is necessary to
829 discuss Mg separation processes. Redistribution of chemical constituents can occur
830 through (1) seawater freezing (Marion and Farren, 1999; Hara et al., 2012), and (2)
831 phase transformation by deliquescence and efflorescence (e.g., Ge et al., 1998; Wise et
832 al., 2009, Woods et al., 2010). Sea-salt fractionation in seawater freezing depends on the
833 temperature (Marion and Farren, 1999; Hara et al., 2012). The air temperature on the
834 Antarctic plateau was often below -30 °C even during summer, as presented in Fig. 2
835 and previous investigations (King, Argentini and Anderson, 2006; Hirasawa et al., 2013).
836 Air temperature might constitute an important condition for some sea-salt precipitation
837 (e.g., ca. -34 °C and -36 °C for KCl and $MgCl_2$ 12 H_2O), as discussed by Marion and
838 Farren (1999). Unlike sea-salts in seawater, however, sea-salts in snow on the Antarctic
839 content were supplied solely by deposition of sea-salt particles that had been transported
840 from coastal regions. When Mg separation is controlled only by lower temperatures,
841 Mg-free sea-salt particles, Mg-rich sea-salt particles, and Mg-rich sulfate particles can

842 be present in the Antarctic regions. However, Mg-free sea-salt particles were not
843 observed over Syowa Station during winter in the air masses transported from the
844 continent and coastal regions (Hara et al., 2013). This result implies that Mg separation
845 was controlled not only by lower air temperature but also by other factors.
846
847 Figure 2 show that the air temperature near the surface had diurnal change also in
848 continental areas. Furthermore, strong diurnal change of air temperatures and solar
849 radiation engender water sublimation on the snow surface of the Antarctic continent
850 (e.g., Kameda et al., 1997; Motoyama et al., 2005). With strong diurnal change of the air
851 temperature, the relative humidity might exhibit a diurnal change near the snow surface
852 on the Antarctic continent during summer. Actually, relative humidity reached ca. 100%
853 during the local night time and reached a minimum in the afternoon at Kohnen Station
854 during summer (Van As et al., 2005). The diurnal variation of the relative humidity can
855 engender (1) phase transformation by deliquescence of available sea-salts on surface
856 snow, (2) condensation and re-freezing of water vapor (e.g., formation of surface hoar)
857 during local night time, and (3) enhancement of quasi-liquid layer and super-cold liquid
858 on the surface snow. Laboratory experiments conducted for earlier studies (e.g., Ge et
859 al., 1998; Wise et al., 2009, Woods et al., 2010) revealed that chemical constituents with
860 lower deliquescence relative humidity (DRH) can be localized in the outer layer
861 (surface) around a solid core through phase transformation by deliquescence. Although

862 relative humidity was minimal in the afternoon at Kohnen Station (Van As et al., 2005),
863 the minimum relative humidity (~89%) was often higher than the deliquescence relative
864 humidity (DRH) of plausible sea-salts. Some examples are the following: NaCl, 75%
865 (Tang and Munkelwitz, 1993); Na_2SO_4, 84% (Tang and Munkelwitz, 1994); $NaNO_3$,
866 75% (Tang and Munkelwitz, 1994); $MgCl_2$ $6H_2O$, 33% (Kelly and Wexler, 2005);
867 $MgSO_4$, 42% (Wang et al., 2008); and KCl, 84% (Tang, 1980). Most plausible sea-salts
868 can be wholly deliquescent even under minimum relative humidity (~89%) on the
869 Antarctic continent. Therefore, phase transformation by deliquescence/efflorescence
870 might not be key processes for Mg separation. With diurnal features of air temperature
871 and relative humidity, re-condensation of water vapor on the snow surface during the
872 local night time might induce enhancement of super-cold water in nanometer-to-
873 micrometer scales, quasi-liquid layer, and re-freezing of water vapors and super-cold
874 water such as hoar formation. Particularly, re-freezing processes on surface snow might
875 cause sea-salt fractionation as well as seawater freezing. Therefore, we propose that the
876 repetition of a diurnal cycle of relative humidity and water sublimation under colder
877 conditions can engender Mg separation on the surface snow on the Antarctic continent
878 during summer.
879

880 **4 Concluding remarks**

881 Measurements of aerosol size distribution and direct aerosol sampling were made in the

Queen Maud Land, Antarctica during the JASE traverse from 14 November 2007 until 24 January 2008. The OPC measurements revealed that aerosol number concentrations decreased gradually with latitude under background conditions (without drifting snow or strong winds) on the Antarctic continent during summer. The estimated aerosol mass concentrations in the size range larger than 0.3 μm were 0.04–5.7 μg m^{-3}. When strong winds and drifting snow occurred, aerosol number concentrations increased precipitously, especially in coarse mode. Air masses were isolated from the Antarctic coasts during the prior 5 days. Therefore, coarse aerosol particles (mainly sea-salt particles) might be released from the snow surface by blowing winds.

Single-particle analysis using SEM-EDX revealed that major aerosol particles were sea-salt particles, modified sea-salt particles, and sulfate particles in coarse mode, and that the sulfate particles and modified sea-salt particles were dominant in fine mode during the JASE traverse. The K-rich sulfates, Mg-rich sulfates, Ca-rich sulfates, and minerals were minor aerosol constituents in coarse and fine modes. Although SO_4^{2-} and $CH_3SO_3^-$ contributed to sea-salt fractionation in coarse and fine modes over Syowa Station during summer (Hara et al., 2005, 2013), sea-salt particles were modified greatly with SO_4^{2-} and NO_3^- in coarse mode, and dominantly with SO_4^{2-} in fine mode in this study. Precursors of particulate NO_3^- (e.g., HNO_3, and NO_x) might have originated from photochemical recycle of NO_3^- in surface snow and subsequent oxidation in the

atmosphere. Median atomic ratios of Mg/Na in sea-salt particles and modified sea-salt particles in coarse and fine modes were often higher than the bulk seawater ratio. In addition, Mg-free sea-salt particles were identified on the Antarctic continent. Because the Mg/Na ratio cannot be changed by sea-salt modification, the presence of Mg-rich sea-salt particles, Mg-free sea-salt particles, and Mg-rich sulfate particles might be associated with sea-salt fractionation. Mg-free sea-salt particles in coarse mode were often identified under conditions with strong winds and drifting snow. Therefore, fractionated sea-salt particles were likely to have been released from the snow surface. This study proposed and assessed the hypothesis that sea-salt fractionation (Mg separation in sea-salts) occurs in surface snow on the Antarctic continent.

Acknowledgments

The JASE traverse was organized by several organizations both in Sweden and Japan. The National Institute of Polar Research (NIPR), Tokyo and the Swedish Polar Research Secretariat (SPRS) managed the logistics in Antarctica. Science management was a collaborative effort of NIPR, Stockholm University, the Royal Institute of Technology in Stockholm and individuals from several universities and institutes in Japan. The JASE traverse is one research project undertaken by the Japanese Antarctic Research Expedition “Studies on systems for climate change and ice sheet change, by introducing new observational methods and technologies”. We thank JARE48 wintering members

922 and JARE49 members for logistic support of the JASE traverse. Special thanks are
923 extended to the logistics members, S. Gunnarsson, H. Kaneko, T. Karlberg, P. Ljusberg
924 and K. Taniguchi and the medical doctors, S. Eriksson and N. Shiga, for their very
925 generous support during the traverse. This research was supported by the Swedish
926 Research Council (VR) and by a Grant-in-Aid for Scientific Research (A) 20241007
927 from the Japan Society for the Promotion of Science (JSPS).

928

929 **References**

930 Allison, I.: Surface climate of the interior of the Lambert Glacier basin, Antarctica, from
931 automatic weather station data, Annals Glaciol., 27, 515–520, 1998.
932 Artaxo, P., Rabello, M. L. C., Maenhaut, W., and van Grieken, R.: Trace elements and
933 individual particle analysis of atmospheric aerosols from the Antarctic Peninsula,
934 Tellus, 44, 318–334, 1992.
935 Bertler, N., Mayewski, P. A., Aristarain, A., Barrett, P., Becagli, S., Bernardo, R. T.,
936 Cunde, X., Curran, M., Dahe, Q., Dixon, D., Ferron, F. A., Fischer, H., Frey, M.,
937 Frezzoi, M., Fundel, F., Genthon, C., Gragani, R., Hamilton, G., Handley, M., Hong,
938 S., Isaksson, E., Jiawen, R., Kamiyama, K., Kanamori, S., Karkas, E., Karlöf, L.,
939 Kaspari, S., Kreutz, K., Kurbatov, A., Meyerson, E., Motoyama, H., Mulvaney, R.,
940 Mingjun, Z., Oerter, H., Osterberg, E., Proposito, M., Pyne, A., Ruth, U., Simoes, J.
941 C., Smith, B., Sneed, S., Teinila, K., Traufetter, F., Udisti, R., Virkkula, A.,

942 Watanabe, O., Williamson, B., Wolff, E., and Zhongqin, L.: Snow Chemistry
943 Across Antarctica, Annals of Glaciology, 41, 167–179, 2005.
944 Bartels-Rausch, T., Jacobi, H.-W., Kahan, T.F., Thomas, J.L., Thomson, E.S., Abbatt,
945 J.P.D., Ammann, M., Blackford, J.R., Bluhm, H., Boxe, C., Domine, F., Frey, M.M.,
946 Gladich, I., Guzmán, M.I., Heger, D., Huthwelker, T., Klán, P., Kuhs, W.F., Kuo,
947 M.H., Maus, S., Moussa, S.G., McNeill, V.F., Newberg, J.T., Pettersson, J.B.C.,
948 Roeselová, M., Sodeau, J.R., 2014. A review of air–ice chemical and physical
949 interactions (AICI): liquids, quasi-liquids, and solids in snow. Atmospheric
950 Chemistry and Physics, *14*, doi:10.5194/acp-14-1587-2014.
951 Bodhaine, B. A.: Aerosol absorption measurements at Barrow, Mauna Loa and the
952 South Pole, J. Geophys. Res., 100, 8967–8975, 1995.
953 Davis, D., Nowak, J. B., Chen, G., Buhr, M., Arimoto, R., Hogan, A., Eisele, F.,
954 Mauldin, L., Tanner, D., Shetter, R., Lefer, B., and McMurry, P.: Unexpected high
955 levels of NO observed at South Pole, Geophys. Res. Lett., 28(19), 3625–3628, 2001.
956 Davis, D., Chen, G., Buhr, M., Crawford, J., Lenschow, D., Lefer, B., Shetter, R., Eisele,
957 F., Mauldin, L., and Hogan, A.: South Pole NOx chemistry: an assessment of
958 factors controlling variability and absolute levels, Atmos. Environ., 38, 5375–5388,
959 2004.
960 Delmonte, B., Petit, J.R., Andersen, K.K., Basile-Doelsch, I., Maggi, V., Ya Lipenkov,
961 V.: Dust size evidence for opposite regional atmospheric circulation changes over

962 east Antarctica during the last climatic transition, Climate Dynamics, 23, 427-438,
963 2004 (doi: 10.1007/s00382-004-0450-9).
964 Delmonte, B., Petit, J. R., Basile-Doelsch, I., Jagoutz, E., Maggi, V.: Late quaternary
965 interglacials in East Antarctica from ice-core dust records, In: Frank Sirocko,
966 Martin Claussen, María Fernanda Sánchez Goñi and Thomas Litt, Editor(s),
967 Developments in Quaternary Sciences, Elsevier, 2007, Volume 7, Pages 53-73,
968 ISSN 1571-0866, ISBN 9780444529558, 2007.
969 Dibb, J., Huey, L., Slusher, D., and Tanner, D.: Soluble reactive nitrogen oxides at South
970 Pole during isCAT 2000, Atmos. Environ., 38, 5399–5409,
971 doi:10.1016/j.atmosenv.2003.01.001, 2004.
972 Ding, Z. J., Li, Y. G., Zeng, R. G., Mao, S. F., Zhang, P., and Zhang, Z. M.: Depth
973 distribution functions of secondary electron production and emission, J. Surface
974 Anal., 15, 249 – 253, 2009.
975 Draxler, R.R. and Rolph, G. D.: HYSPLIT (HYbrid Single-Particle Lagrangian
976 Integrated Trajectory) Model access via NOAA ARL READY Website
977 (http://ready.arl.noaa.gov/HYSPLIT.php). NOAA Air Resources Laboratory, Silver
978 Spring, MD, 2013.
979 Eisele, F., Davis, D. D., Helmig, D., Oltmans, S. J., Neff, W., Huey, G., Tanner, D., Chen,
980 G., Crawford, J., Arimoto, R., Buhr, M., Mauldin, L., Hutterli, M., Dibb, J., Blake,
981 D., Brooks, S. B., Johnson, B., Roberts, J. M., Wang, Y., Tan, D., and Flocke, F.:

982 Antarctic Tropospheric Chemistry Investigation (ANTCI) 2003 overview, Atmos.
983 Environ., 42, 2749-2761, (doi.org/10.1016/j.atmosenv.2007.04.013), 2008.
984 Frey, M. M., Savarino, J., Morin, S., Erbland, J., and Martins, J. M. F.: Photolysis
985 imprint in the nitrate stable isotope signal in snow and atmosphere of East
986 Antarctica and implications for reactive nitrogen cycling, Atmos. Chem. Phys., 9,
987 8681–8696, doi:10.5194/acp-9-8681-2009, 2009.
988 Fujita, S., Holmlund, P., Andersson, I., Brown, I., Enomoto, H., Fujii, Y., Fujita, K.,
989 Fukui, K., Furukawa, T., Hansson, M., Hara K., Hoshina, Y., Igarashi, M., Iizuka, Y.,
990 Imura, S., Ingvander, S., Karlin, T., Motoyama, H., Nakazawa, F., Oerter, H.,
991 Sjöberg, L., Sugiyama, S., Surdyk, S., Ström, J. Uemura, R. and Wilhelms, F.,
992 Spatial and temporal variability of snow accumulation in Dronning Maud Land,
993 East Antarctica, including two deep ice coring sites at Dome Fuji and EPICA DML,
994 ***The Cryosphere,*** 5, 1057-1081, 2011 (doi:10.5194/tc-5-1057-2011).
995 Fujita, S., Fukui, K., Nakazawa, F., Enomoto, H., and Sugiyama, S.: Report of the
996 Japanese-Swedish joint Antarctic traverse: II. Report of field expedition in
997 2007/2008 season, Submitted to Antarctic record (in Japanese with English
998 abstract).
999 Ge, Z., Wexler, A. S., and Johnston, M. V.: Deliquescence Behavior of Multicomponent
1000 Aerosols, *The Journal of Physical Chemistry A* 1998 *102* (1), 173-180
1001 Geilfus, N.-X., R. J. Galley, M. Cooper, N. Halden, A. Hare, F. Wang, D. H. Søgaard,

and S. Rysgaard: Gypsum crystals observed in experimental and natural sea ice, Geophysical Research Letters, 40, doi:10.1002/2013GL058479, 2013.

Goldstein, J. I., Newbury, D. E., Joy, D. C., Lyman, C. E., Echlin, P., Lifshin, E., Sawyer, L., and Michael, J.: Chapter 6 Generation of X-rays in the SEM specimen, in "Scanning Electron Microscopy and X-ray Micronalysis, 3rd ed", p. 271-296, Plenum Press, New York, 2003.

Hara, K., Kikuchi, T., Furuya, K., Hayashi, M., and Fujii, Y.: Characterization of Antarctic aerosol particles using laser microprobe mass spectrometry, Environ. Sci. Technol., 30(2), 385–391, 1995.

Hara, K., Osada, K., Nishita, C., Yamagata, S., Yamanouchi, T., Herber, A., Matsunaga, K., Iwasaka, Y., Nagatani, M., and Nakata, H.: Vertical variations of sea-salt modification in the boundary layer of spring Arctic during the ASTAR 2000 campaign, Tellus, 54B, 361–376, 2002.

Hara, K., Osada, K., Kido, M., Hayashi, M., Matsunaga, K., Iwasaka, Y., Yamanouchi, T., Hashida, G., and Fukatsu, T.: Chemistry of sea-salt particles and inorganic halogen species in the Antarctic regions: Compositional differences between coastal and inland stations, J. Geophys. Res., 109, D20208, doi:10.1029/2004JD004713, 2004.

1020 Hara, K., Osada, K., Kido, M., Matsunaga, K., Iwasaka, Y., and Hashida, G.: Seasonal
1021 variations of sea-salt constituents and sea-salt modification at Syowa station,
1022 Antarctica, Tellus, 57B, 230-246, 2005.
1023 Hara, K., Osada, K., Yabuki, M., Hashida, G., Yamanouchi, T., Hayashi, M., Shiobara,
1024 M., Nishita-Hara, C., and Wada, M.: Haze episodes at Syowa Station, coastal
1025 Antarctica: Where did they come from?, J. Geophys. Res., 115, D14205,
1026 doi:10.1029/2009JD012582, 2010a.
1027 Hara, K., Hirasawa, N., Yamanouchi, T., Wada, M., Herber, A., and ANTSYO-II
1028 members, Spatial distributions and mixing states of aerosol particles in the summer
1029 Antarctic troposphere, Antarctic Record, 54, 704-730, 2010 (in Japanese with
1030 English abstract).
1031 Hara, K., Osada, K., Nishita-Hara, C., Yabuki, M., Hayashi, M., Yamanouchi, T., Wada,
1032 M., and Shiobara, M.: Seasonal features of ultra-fine particle volatility in coastal
1033 Antarctic troposphere, Atmos. Chem. Phys., 11, 9803–9812, doi:10.5194/acp-11-
1034 9803-2011, 2011a.
1035 Hara, K., Osada, K., Nishita-Hara, C., and Yamanouchi, T.: Seasonal variations and
1036 vertical features of aerosol particles in the Antarctic troposphere, Atmos. Chem.
1037 Phys., 11, 5471–5484, doi:10.5194/acp-11-5471-2011, 2011b.
1038 Hara, K., Osada, K., Yabuki, M., and Yamanouchi, T.: Seasonal variation of fractionated
1039 sea-salt particles on the Antarctic coast, Geophys. Res. Lett., 39, L18801,

doi:10.1029/2012GL052761, 2012.

Hara, K., Osada, and Yamanouchi, T.: Tethered balloon-borne aerosol measurements: Seasonal and vertical variations of aerosol constituents over Syowa Station, Antarctica, Atmos. Chem. Phys., 13, 9119-9139, doi:10.5194/acp-13-9119-2013, 2013.

Helmig, D., Johnson, B., Warshawsky, M., Morse, T., Neff, W., Eisele, F., and Davis, D. D.: Nitric Oxide in the Boundary-Layer at South Pole during the Antarctic Tropospheric Chemistry Investigation (ANTCI). Atmos. Environ., 42, 2817-2830, 2008.

Hirasawa, N., Nakamura, H., Motoyama, H., Hayashi, M., and Yamanouchi, T.: The role of synoptic-scale features and advection in prolonged warming and generation of different forms of precipitation at Dome Fuji station, Antarctica, following a prominent blocking event, J. Geophys. Res. Atmos., 118, doi:10.1002/jgrd.50532, 2013.

Huey, L.G., Tanner, D. J., Slusher, D. L., Dibb, J. E., Arimoto, R., Chen, G., Davis, D., Buhr, M. P., Nowak, J. B., Mauldin III, R. L., Eisele, F. L., and Kosciuch, E.: CIMS measurements of HNO_3 and SO_2 at the South Pole during ISCAT 2000, Atmospheric Environment, 38, 5411-5421, 2004 (doi.org/10.1016/j.atmosenv.2004.04.037), 2004.

Iizuka, Y., Tsuchimoto, A., Hoshina, Y., Sakurai, T., Hansson, M., Karlin, T., Fujita, K., Nakazawa, F., Motoyama, H., and Fujita, S.: The rates of sea salt sulfatization in the

1060 atmosphere and surface snow of inland Antarctica, J. Geophys. Res., 117, D04308,
1061 doi:10.1029/2011JD016378, 2012.
1062 Jones, A. E., Wolff, E. W., Ames, D., Bauguitte, S. J.-B., Clemitshaw, K. C., Fleming, Z.,
1063 Mills, G. P., Saiz-Lopez, A., Salmon, R. A., Sturges, W. T., and Worton, D. R.: The
1064 multi-seasonal NO_y budget in coastal Antarctica and its link with surface snow and
1065 ice core nitrate: results from the CHABLIS campaign, Atmos. Chem. Phys., 11,
1066 9271-9285, doi:10.5194/acp-11-9271-2011, 2011
1067 Jourdain, B. and Legrand, M.: Seasonal variations of atmospheric dimethylsulfide,
1068 dimethylsulfoxide, sulfur dioxide, methanesulfonate, and non-sea-salt sulfate
1069 aerosols at Dumont d'Urville (coastal Antarctica) (December 1998 to July 1999), J.
1070 Geophys. Res., 106(D13), 14391–14408, 2001.
1071 Jourdain, B., and Legrand, M.: Year-round records of bulk and size-segregated aerosol
1072 composition and HCl and HNO_3 levels in the Dumont d'Urville (coastal Antarctica)
1073 atmosphere: Implications for sea-salt aerosol fractionation in the winter and summer,
1074 J. Geophys. Res., 107(D22), 4645, doi:10.1029/2002JD002471, 2002.
1075 Junge, C. E.: Aerosols in "Air chemistry and radioactivity" Academic Press., 111–208,
1076 1963.
1077 Kameda, T., Azuma, N., Furukawa, T., Ageta, Y., and Takahashi, S.: Surface mass
1078 balance, sublimation and snow temperatures at Dome Fuji Station, Antarctica, in
1079 1995, Proc. NIPR Symp. Polar Meteorol. Glaciol., 11, 24–34, 1997.

1080 Kelly, J. T., and Wexler, A. S.: Thermodynamics of carbonates and hydrates related to
1081 heterogeneous reactions involving mineral aerosol, J. Geophys. Res., 110, D11201,
1082 doi:10.1029/2004JD005583, 2005.
1083 Kerminen, V. M., Teinilä, K., and Hillamo, R.: Chemistry of sea-salt particles in the
1084 summer Antarctic atmosphere, Atmos. Environ., 34, 2817–2825, 2000.
1085 King, J. C., Argentini, S. A., and Anderson, P. S.: Contrasts between the summertime
1086 surface energy balance and boundary layer structure at Dome C and Halley stations,
1087 Antarctica, J. Geophys. Res., 111, D02105, doi:10.1029/2005JD006130, 2006.
1088 Legrand, M., Sciare, J., Jourdain, B., and Genthon, C.: Subdaily variations of
1089 atmospheric dimethylsulfide, dimethylsulfoxide, methanesulfonate, and non-sea-salt
1090 sulfate aerosols in the atmospheric boundary layer at Dumont d'Urville (coastal
1091 Antarctica) during summer, J. Geophys. Res., 106(D13), 14,409–14,422, 2001.
1092 Legrand, M., Preunkert, S., Jourdain, B., and Aumont, B.: Year-round records of gas and
1093 particulate formic and acetic acids in the boundary layer at Dumont d'Urville,
1094 coastal Antarctica. J. Geophys. Res., 109 109, D06313, doi:10.1029/2003JD003786,
1095 2004.
1096 Marion, G. M., and Farren, R. E.: Mineral solubilities in the Na-K-Mg-Ca-Cl-SO_4-H_2O
1097 system: a re-evaluation of the sulfate chemistry in the Spencer-Møller-Weare model,
1098 Geochim. Cosmochim. Acta, Volume 63, 1305-1318, doi.org/10.1016/S0016-
1099 7037(99)00102-7), 1999.

1100 Minikin, A., Legrand, M., Hall, J., Wagenbach, D., Kleefeld, C., Wolff, E., Pasteur, E.,
1101 and Ducroz, F.: Sulfur-containing species (sulfate and methanesulfonate) in coastal
1102 Antarctic aerosol and precipitation, J. Geophys. Res., 103(D9), 10975–10990, 1998.
1103 Motoyama, H., Hirasawa, N., Satow, K., and Watanabe, O.: Seasonal variations in
1104 oxygen isotope ratios of daily collected precipitation and wind drift samples and in
1105 the final snow cover at Dome Fuji Station, Antarctica, J. Geophys. Res., 110,
1106 D11106, doi:10.1029/2004JD004953, 2005.
1107 Mouri, H., Nagao, I., Okada, K., Koga, S., and Tanaka, H.: Individual-particle analyses
1108 of coastal Antarctic aerosols, Tellus, 51B, 603–611, 1999.
1109 Neff, W., Helmig, D., Grachev, A., and Davis, D.: A study of boundary layer behavior
1110 associated with high NO concentrations at the South Pole using a minisodar,
1111 tethered balloon, and sonic anemometer, Atmospheric Environment, 42, 2762-2779,
1112 (doi.org/10.1016/j.atmosenv.2007.01.033), 2008.
1113 Preunkert, S., Jourdain, B., Legrand, M., Udisti, R., Becagli, S., and Cerri, O.:
1114 Seasonality of sulfur species (dimethylsulfide, sulfate, and methanesulfonate) in
1115 Antarctica: Inland versus coastal regions, J. Geophys. Res., 113, D15302,
1116 doi:10.1029/2008JD009937, 2008.
1117 Rankin, A. M., Auld, V., and Wolff, E. W.: Frost flowers as a source of fractionated sea
1118 salt aerosol in the polar regions, Geophys. Res. Lett., 27(21), 3469–3472,
1119 doi:10.1029/2000GL011771, 2000.

1120 Rankin, A. M., Wolff, E. W., and Martin, S.: Frost flowers: Implications for tropospheric
1121 chemistry and ice core interpretation, J. Geophys. Res., 107(D23), 4683,
1122 doi:10.1029/2002JD002492, 2002.
1123 Rankin, A. M. and Wolff, E. W.: A year-long record of size-segregated aerosol
1124 composition at Halley, Antarctica, J. Geophys. Res., 108(D24), 4775,
1125 doi:10.1029/2003JD003993, 2003.
1126 Reijmer, C. H., and M. R. van den Broeke (2001), Moisture source of
1127 precipitation in Western Dronning Maud Land, Antarctica, Antarct. Sci.,
1128 13(2), 210 – 220, doi:10.1017/S0954102001000293.
1129 Reijmer, C. H., M. R. van den Broeke, and M. P. Scheele (2002), Air parcel trajectories
1130 and snowfall related to five deep drilling locations in Antarctica based on the ERA-
1131 15 dataset, J. Clim., 15, 1957 – 1968, doi:10.1175/15200442
1132 (2002)015<1957:APTASR>2.0.CO;2.
1133 Sato, K. and Hirasawa, N.: Statistics of Antarctic surface meteorology based on hourly
1134 data in 1957–2007 at Syowa Station, Polar Sci., 1, 1–15, 2007.
1135 Savoie, D. L., Prospero, J. M., Larsen, R. J., and Saltzman, E. S.: Nitrogen and sulfur
1136 species in aerosols at Mawson, Antarctica, and their relationship to natural
1137 radionuclides, J. Atmos. Chem., 14, 181–204, 1992.
1138 Savoie, D. L., Prospero, J. M., Larsen, R. J., Huang, F., Izaguirre, M. A., Huang, T.,
1139 Snowdon, T. H., Custals, L., and Sanderson, C. G.: Nitrogen and sulfur species in

1140 Antarctic aerosols at Mawson, Palmer Station, and Marsh (King George Island), J.
1141 Atmos. Chem., 17, 95–122, 1993.
1142 Suzuki, K., Yamanouchi, T., Kawamura, K. and Motoyama, H.: The spatial and seasonal
1143 distributions of air-transport origins to the Antarctic based on 5-day backward
1144 trajectory analysis, Polar Science 7, 205-213, 2013.
1145 Teinilä, K., Kerminen, V.-M., and Hillamo, R.: A study of size-segregated aerosol
1146 chemistry in the Antarctic atmosphere, J. Geophys. Res., 105(D3), 3893–3904,
1147 doi:10.1029/1999JD901033, 2000.
1148 Udisti, R., Dayan, U., Becagli, S., Busetto, M., Frosini, D., Legrand, M., Lucarelli, F.,
1149 Preunkert, S., Severi, M., Traversi, R., and Vitale, V.: Sea spray aerosol in central
1150 Antarctica. Present atmospheric behaviour and implications for paleoclimatic
1151 reconstructions, Atmos. Environ., 52, 109–120, 2012.
1152 Van As, D., Van Den Broeke, M., and Van De Wal, R.: Daily cycle of the surface layer
1153 and energy balance on the high Antarctic Plateau, Antarctic Science, 17, 121–133,
1154 2005.
1155 Wagenbach, D., Ducroz, F., Mulvaney, R., Keck, L., Minikin, A., Legrand, M. J., Hall,
1156 S., and Wolff, E. W.: Sea-salt aerosol in coastal Antarctic regions, J. Geophys. Res.,
1157 103(D9), 10,961–10,974, 1998.
1158 Wang, L.-Y., Ding, F., Zhang, Y.-H., Zhao, L.-J. and Hu, Y.-A.: Anomalous hygroscopic
1159 growth of fine particles of $MgSO_4$ aerosols investigated by FTIR/ATR

1160 spectroscopy, Spectrochimica Acta Part A, 71, 682-687,
1161 doi:10.1016/j.saa.2008.01.027, 2008.
1162 Weller, R., Jones, A. E., Wille, A., Jacobi, H.-W., McIntyre, H. P., Sturges, W. T., Huke,
1163 M. and Wagenbach, D.: Seasonality of reactive nitrogen oxides (NOy) at Neumayer
1164 Station, Antarctica. J. Geophys. Res., 107(D23), 4673, doi:10.1029/2002JD002495,
1165 2002.
1166 Weller, R. and Wagenbach, D.: Year-round chemical aerosol records in continental
1167 Antarctica obtained by automatic samplings, Tellus, 59B, 755–765, 2007.
1168 Weller, R., Minikin, A., Wagenbach, D., and Dreiling, V.: Characterization of the
1169 interannual, seasonal, and diurnal variations of condensation particle concentrations
1170 at Neumayer, Antarctica, Atmos. Chem. and Phys., 11, 13243–13257 (doi:
1171 10.5194/acp-11-13243-2011), 2011.
1172 Wilson, T. R.: Salinity and the major elements of sea-water, in Chemical Oceanography,
1173 edited by J. P. Riley and G. Skirrow, pp. 365–413, Academic Press, San Diego,
1174 Calif., 1975.
1175 Wise, M. E., Freney, E. J., Tyree, C. A., Allen, J. O., Martin, S. T., Russell, L. M., and
1176 Buseck P. R.: Hygroscopic behavior and liquid-layer composition of aerosol
1177 particles generated from natural and artificial seawater, J. Geophys. Res., 114,
1178 D03201, doi:10.1029/2008JD010449, 2009.

1179 Woods, E., Chung, D., Lanney, H. M., and Ashwell, B. A.: Surface morphology and
1180 phase transitions in mixed NaCl/$MgSO_4$ aerosol particles, ***J. Phys. Chem. A, 114*** (8),
1181 2837-2844, 2010.
1182 Wouters, L., Artaxo, P., and van Grieken, R.: Laser Microprobe Mass Analysis of
1183 Individual Antarctic Aerosol Particles, Int. J. Environ. Anal. Chem., 38, 427–438,
1184 1990.
1185 Yamato, M., Iwasaka, Y., Ono, A., and Yoshida, M.: On the sulfate particles in the
1186 submicron size range collected at Mizuho Station and in east Queen Maud Land,
1187 Antarctica, Polar Meteorol. Glaciol., 1, 82–90, 1987a.
1188 Yamato, M., Iwasaka, Y., Okada, K., Ono, A., Nishio, F., and Fukabori, M.: Evidence
1189 for the presence of submicron sulfuric acid particles in summer Antarctic
1190 atmosphere: Preliminary results, Proc. NIPR Symp. Polar Meteorol. Glaciol., 1, 74–
1191 81, 1987b.

Figure Captions

Figure 1 Traverse routes of Japanese team during JASE campaign. Black lines represent traverse routes between S16 and Dome F in incoming and outgoing traverse. The blue line represents traverse route from Dome F to meeting point in the incoming traverse. The red line represents traverse route from the meeting point to Dome F in outgoing traverse. The traverse route of the Swedish team was referred from Fujita et al. (2011).

Figure 2 Variations of latitudes, elevation, air temperature, and relative humidity during the JASE traverse. Cyan stars represent dates and locations of aerosol measurements and direct sampling.

Figure 3 5-day backward trajectories from every camp site in (a) incoming traverse from S16 to Dome F, and (b) traverse from Dome F (DF) to meeting point (MP), (c) traverse from meeting point to S16 in outgoing traverse. Black lines show the traverse route. Altitudes denote the height above the ground. Color code corresponds to the latitude at starting points of the trajectory.

Figure 4 Horizontal features of air temperature, elevation, wind speed, aerosol number concentrations and Junge slope during incoming traverse from S16 to the meeting point. Red boxes show conditions with drifting snow.

Figure 5 Horizontal features of air temperature, elevation, wind speed, aerosol number concentrations and Junge slope during outgoing traverse from the meeting point to S16. Red boxes show conditions with drifting snow.

Figure 6 SEM images of aerosol particles in (a) coarse mode and (b) fine mode.

Figure 7 EDX spectra of aerosol particles collected during the JASE traverse. Asterisks denote background peaks derived from the sample substrate.

Figure 8 Horizontal features of relative abundance of each aerosol constituent in (a–b) coarse and (c–d) fine modes during the incoming traverse.

Figure 9 Horizontal features of relative abundance of each aerosol constituent in (a–b) coarse and (c–d) fine modes during the outgoing traverse.

Figure 10 Ternary plots (Na–S–Cl) of sea-salt particles in coarse and fine modes during the JASE traverse. Red, and blue stars respectively denote atomic ratios of (1) bulk seawater, and (2) wholly Cl depleted sea-salt particles with sulfates. Black lines represent stoichiometric lines among constituents.

Figure 11 Horizontal features of atomic ratio of Cl/Na and S/Na in coarse and fine modes during the incoming traverse. In box plots, the top bar, top box line, black middle box line, bottom box line, and bottom bar respectively denote values of 90%, 75%, 50% (median), 25%, and 10%. The red line shows mean values.

Figure 12 Horizontal features of atomic ratio of Cl/Na and S/Na in coarse and fine modes during the outgoing traverse. In box plots, the top bar, top box line, black middle box line, bottom box line, and bottom bar respectively denote values of 90%, 75%, 50% (median), 25%, and 10%. The red line shows mean values.

Figure 13 Ternary plots (Na–Mg–S) of sea-salt particles in coarse and fine modes during the JASE traverse. Red, blue, cyan, and green stars respectively denote atomic ratios of (1) bulk seawater, (2) wholly Cl depleted sea-salt particles with sulfates, (3) $MgCl_2$, and (4) $MgSO_4$. Blue, pink, and red lines represent stoichiometric lines among constituents.

1250

1251 Figure 14 Horizontal features of the atomic ratio of Mg/Na in coarse and fine modes
1252 during the incoming traverse. In box plots, the top bar, top box line, black middle
1253 box line, bottom box line, and bottom bar respectively denote values of 90%, 75%,
1254 50% (median), 25%, and 10%. The red line shows mean values.

1255

1256

1257

Fig. 1

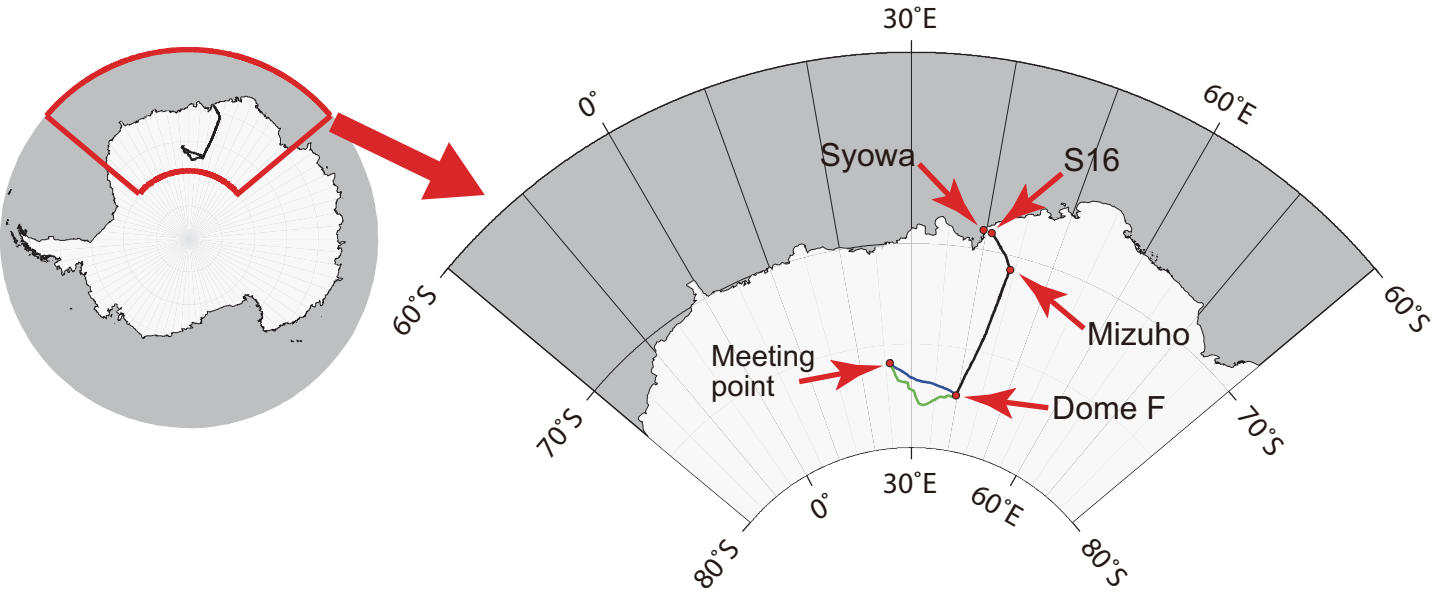
30˚E
0˚
60˚E
Syowa
S16
60˚S
Mizuho
Meeting
point
Dome F
70˚S
70˚S
0˚
30˚E
60˚E
80˚S
80˚S

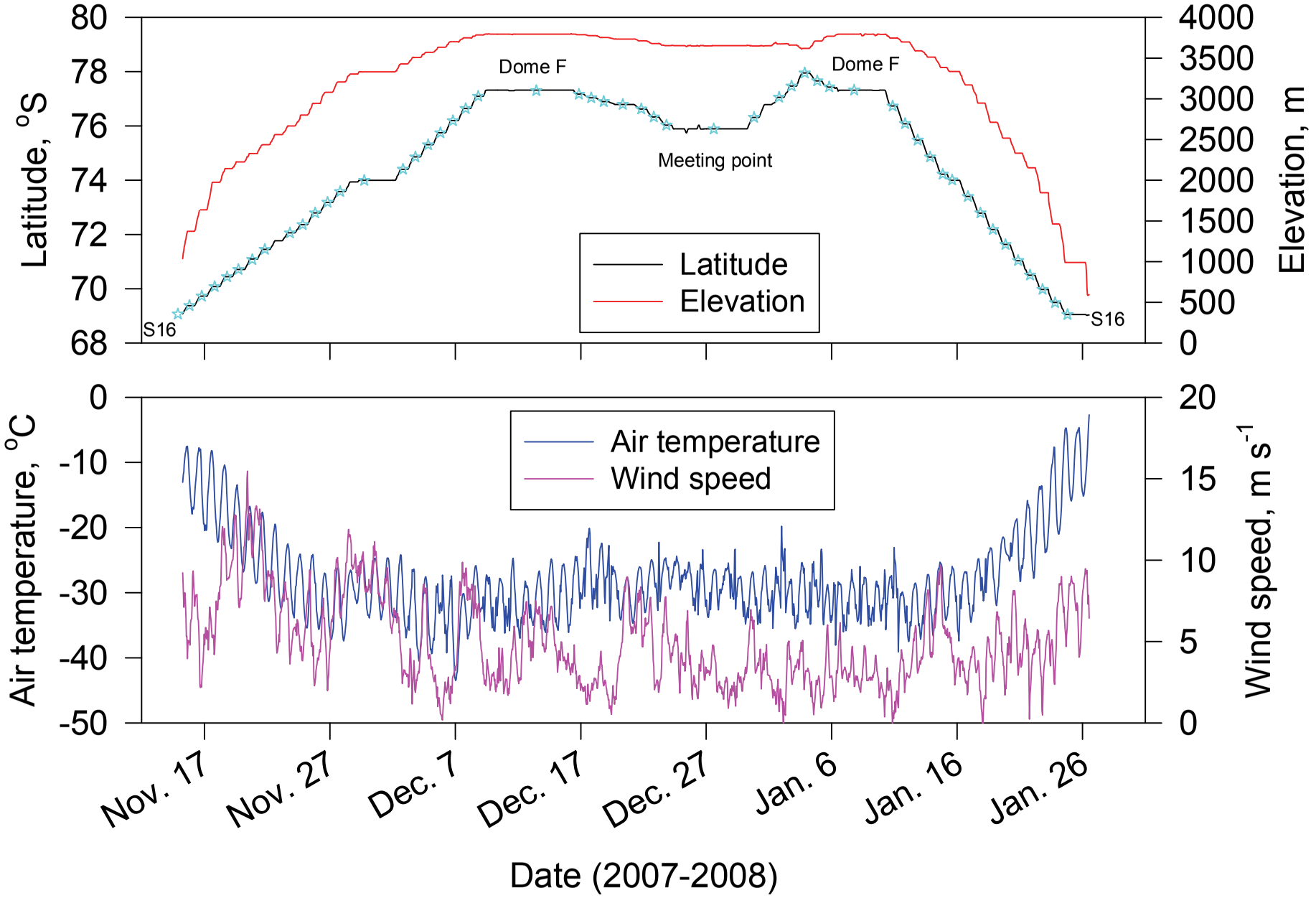
Latitude, °S
Elevation, m
Dome F
Dome F
Meeting point
S16
S16
Latitude
Elevation
Air temperature, °C
Wind speed, m s-1
Air temperature
Wind speed
Nov. 17
Nov. 27
Dec. 7
Dec. 17
Dec. 27
Jan. 6
Jan. 16
Jan. 26
Date (2007-2008)

Fig. 2

Fig.3a

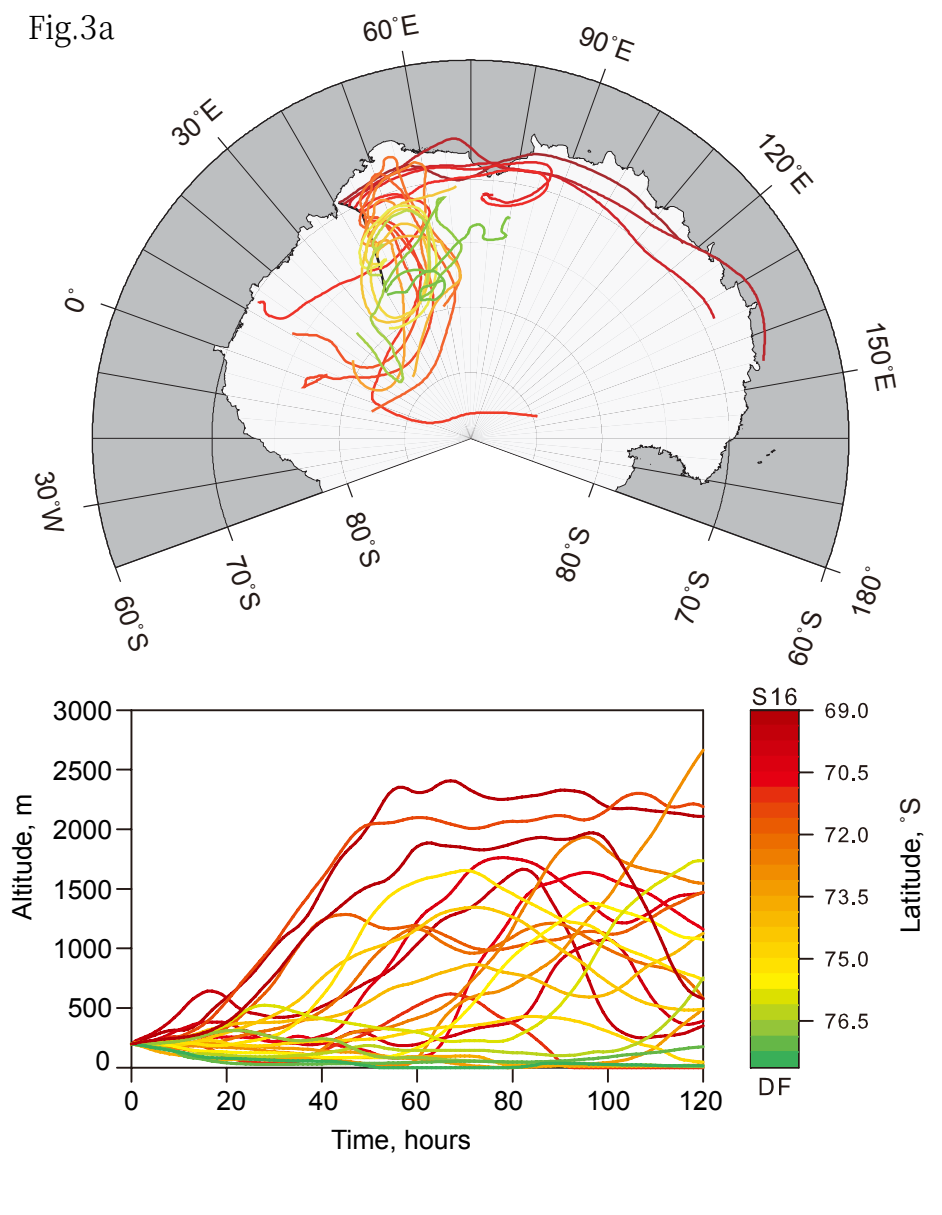
60˚E
90˚E
30˚E
120˚E
0˚
150˚E
30˚W
80˚S
70˚S
80˚S
70˚S
60˚S
60˚S
180˚
3000
2500
2000
1500
1000
500
0
Altitude, m
0
20
40
60
80
100
120
Time, hours
S16
69.0
70.5
72.0
73.5
75.0
76.5
DF
Latitude, ˚S

Fig.3b

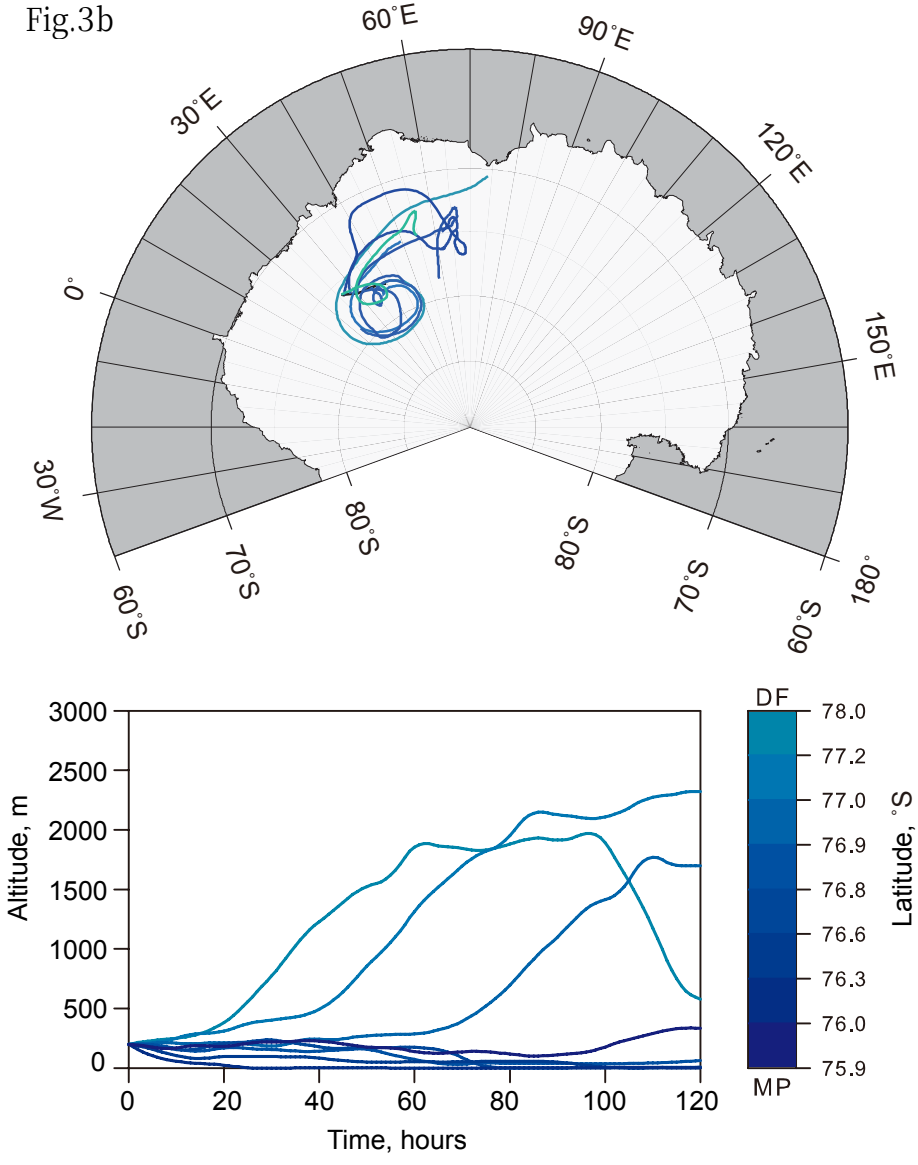
60°E
90°E
30°E
120°E
0°
150°E
30°W
80°S
80°S
70°S
70°S
60°S
60°S
180°
3000
2500
2000
1500
1000
500
0
Altitude, m
0
20
40
60
80
100
120
Time, hours
DF
78.0
77.2
77.0
76.9
76.8
76.6
76.3
76.0
75.9
MP
Latitude, °S

Fig.3c

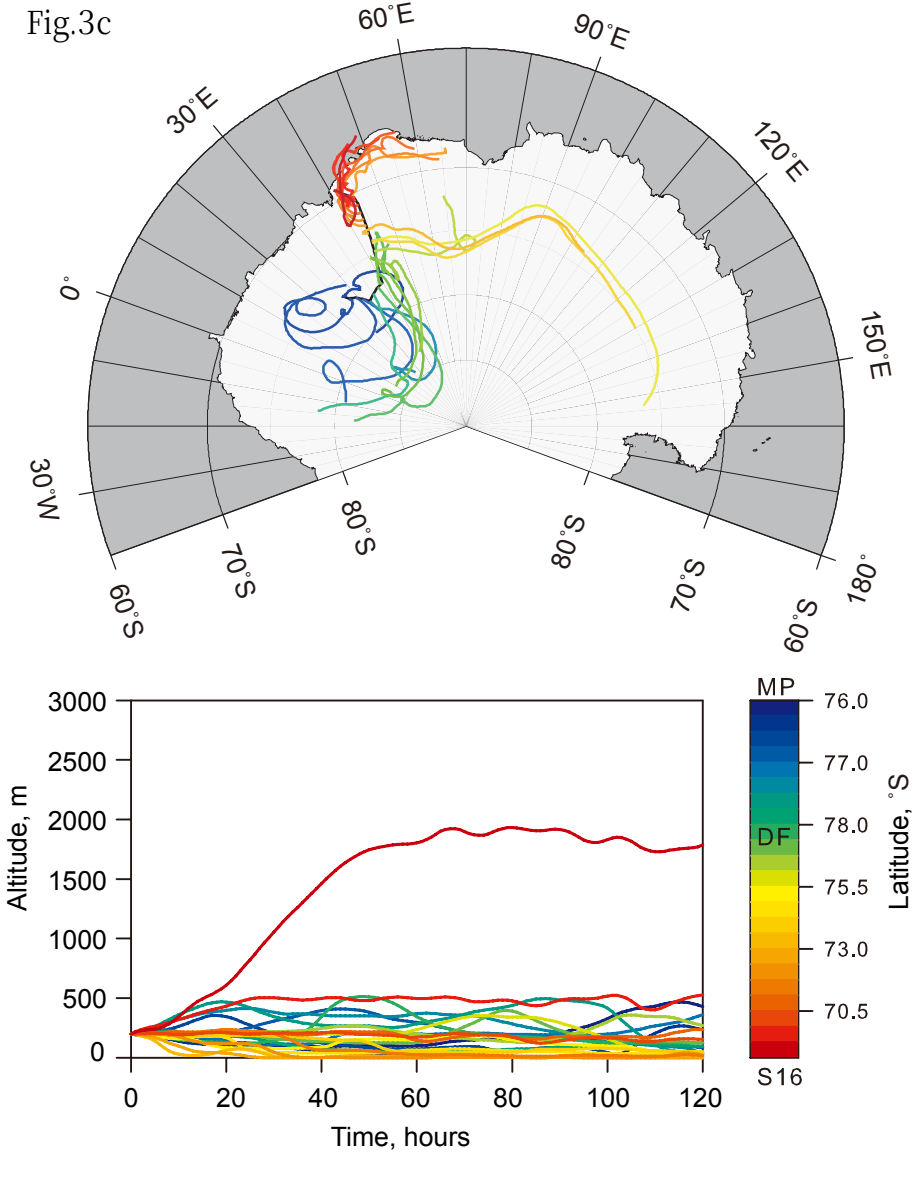
60˚E
90˚E
30˚E
120˚E
0˚
150˚E
30˚W
80˚S
70˚S
60˚S
80˚S
70˚S
60˚S
180˚
3000
2500
2000
1500
1000
500
0
Altitude, m
0
20
40
60
80
100
120
Time, hours
MP
DF
S16
76.0
77.0
78.0
75.5
73.0
70.5
Latitude, ˚S

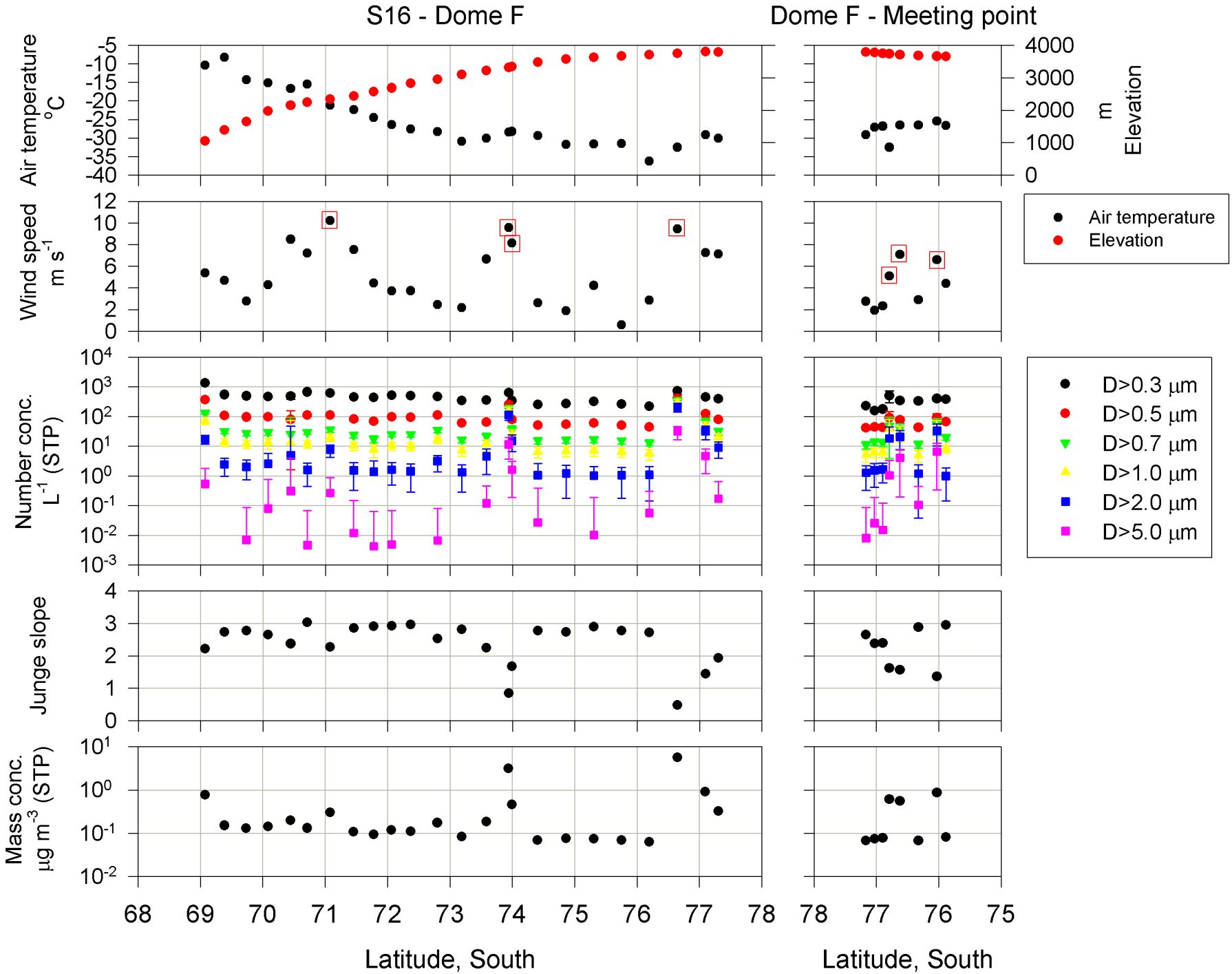
S16 - Dome F
Dome F - Meeting point
Air temperature °C
Elevation m
Wind speed m s-1
Number conc. L-1 (STP)
Junge slope
Mass conc. µg m-3 (STP)
Air temperature
Elevation
D>0.3 µm
D>0.5 µm
D>0.7 µm
D>1.0 µm
D>2.0 µm
D>5.0 µm
Latitude, South
Latitude, South

Fig. 4

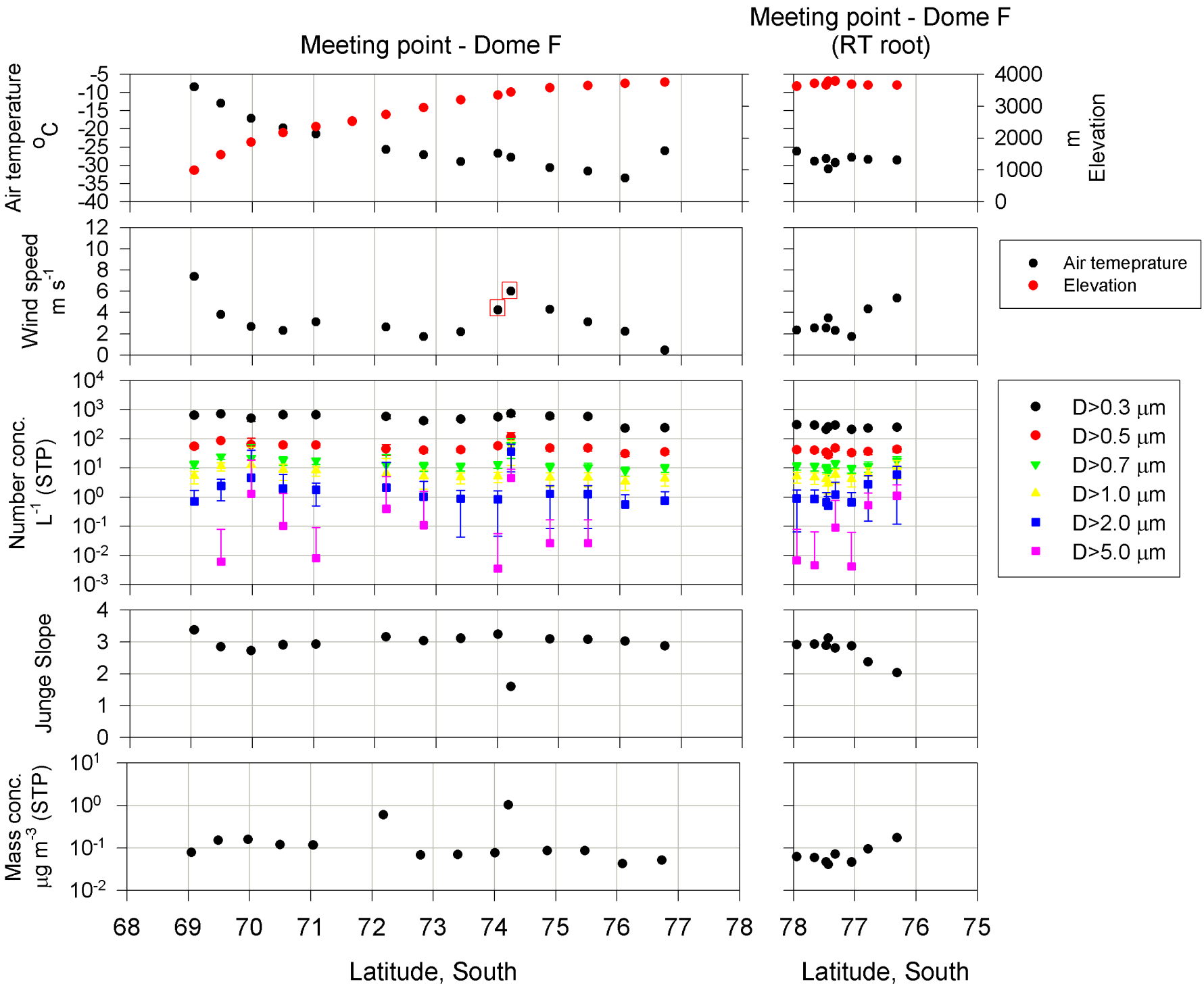
Meeting point - Dome F
Meeting point - Dome F
(RT root)
Air temperature
°C
-5
-10
-15
-20
-25
-30
-35
-40
4000
3000
2000
1000
0
m
Elevation
Wind speed
m s-1
12
10
8
6
4
2
0
Air temeprature
Elevation
Number conc.
L-1 (STP)
10^4
10^3
10^2
10^1
10^0
10^-1
10^-2
10^-3
D>0.3 µm
D>0.5 µm
D>0.7 µm
D>1.0 µm
D>2.0 µm
D>5.0 µm
Junge Slope
4
3
2
1
0
Mass conc.
µg m-3 (STP)
10^1
10^0
10^-1
10^-2
68
69
70
71
72
73
74
75
76
77
78
78
77
76
75
Latitude, South
Latitude, South

Fig. 5

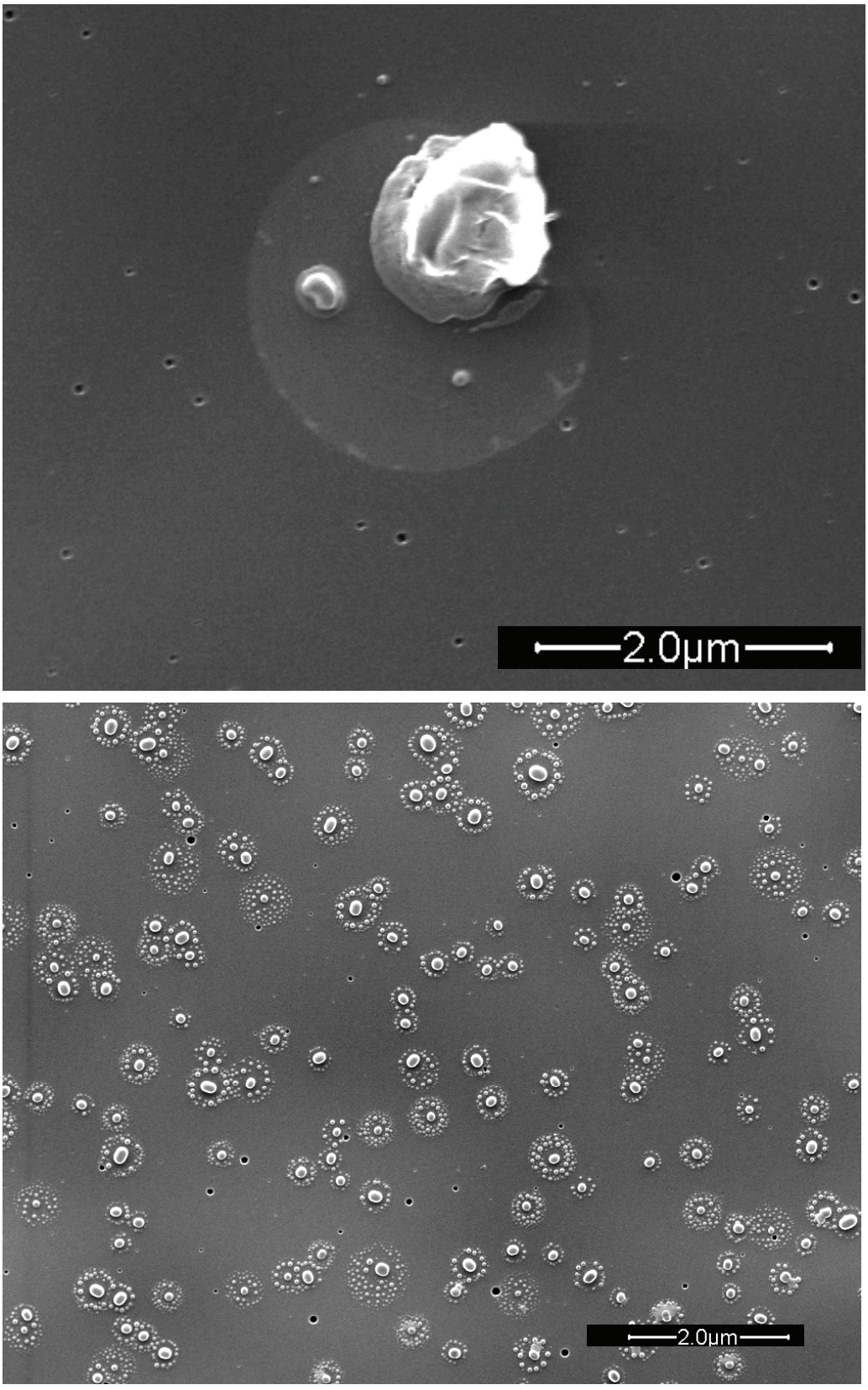

Fig. 6

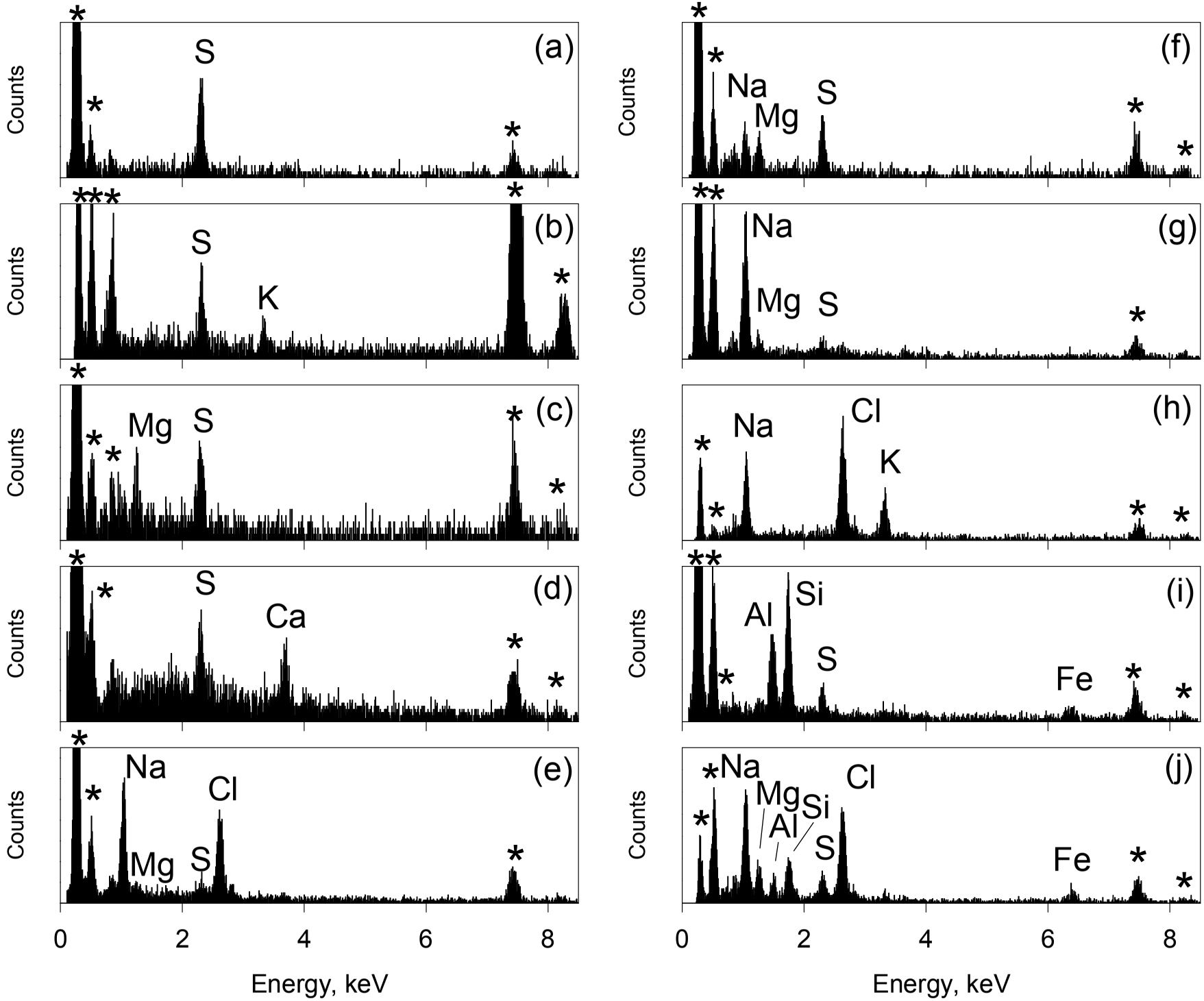
(a)
S
(b)
S
K
(c)
Mg
S
(d)
S
Ca
(e)
Na
Cl
Mg
S
(f)
Na
Mg
S
(g)
Na
Mg
S
(h)
Na
Cl
K
(i)
Al
Si
S
Fe
(j)
Na
Mg
Al
Si
Cl
S
Fe
Counts
0
2
4
6
8
Energy, keV

Fig. 7

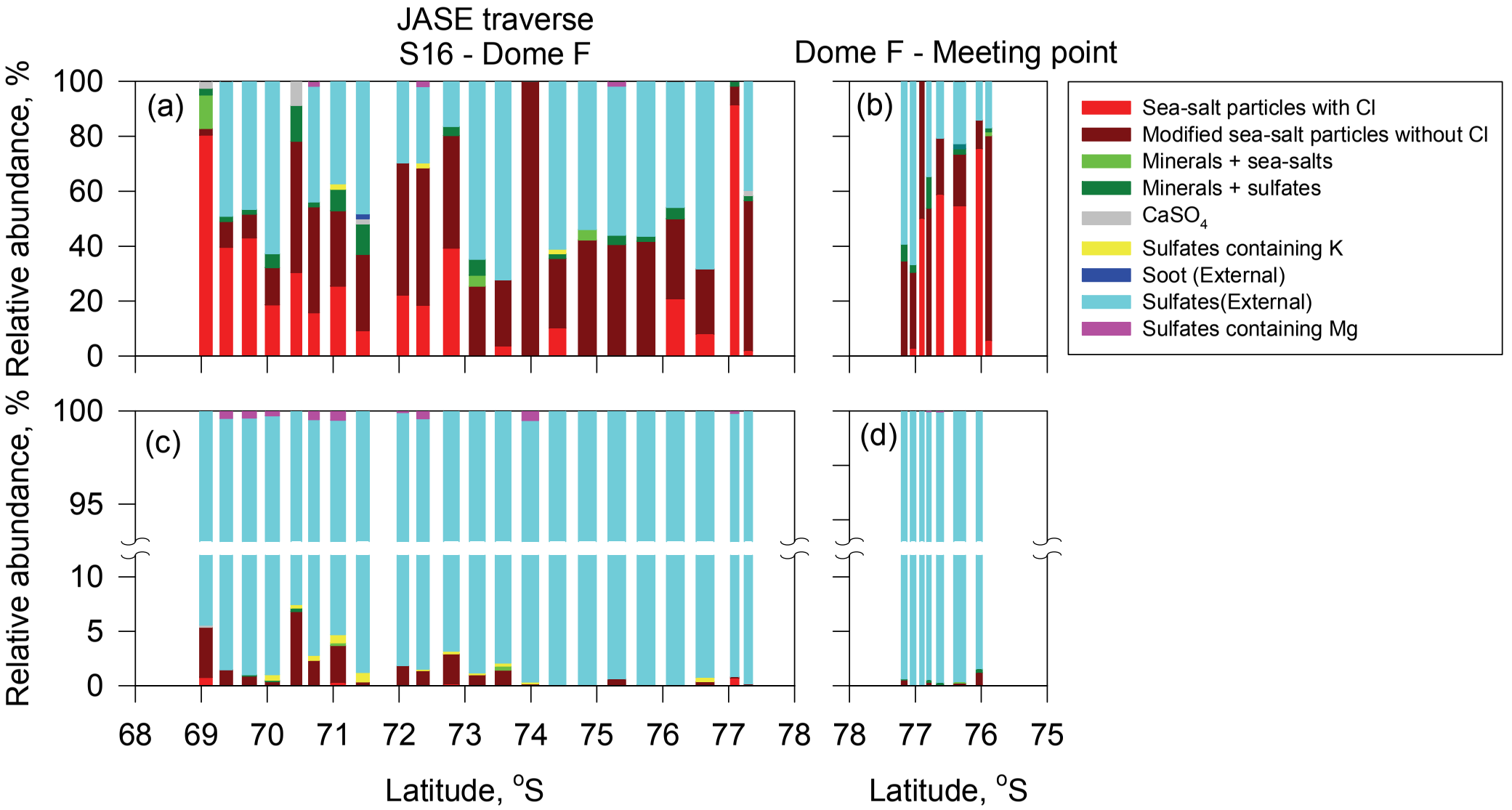
JASE traverse
S16 - Dome F
Dome F - Meeting point
(a)
(b)
(c)
(d)
Relative abundance, %
100
80
60
40
20
0
95
10
5
68
69
70
71
72
73
74
75
76
77
78
Latitude, °S
Sea-salt particles with Cl
Modified sea-salt particles without Cl
Minerals + sea-salts
Minerals + sulfates
CaSO4
Sulfates containing K
Soot (External)
Sulfates(External)
Sulfates containing Mg

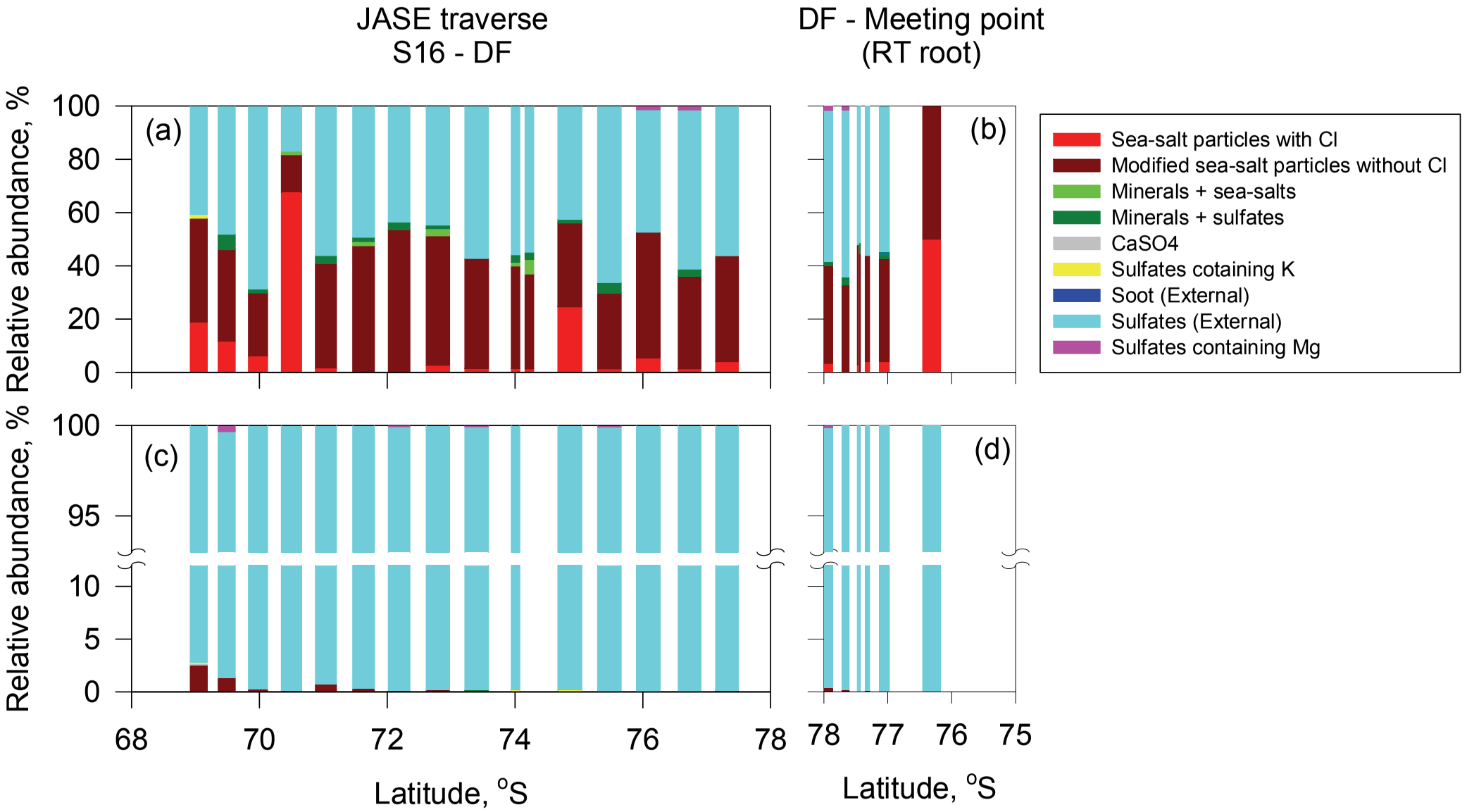
JASE traverse
S16 - DF
DF - Meeting point
(RT root)
(a)
(b)
(c)
(d)
Relative abundance, % Relative abundance, %
100
80
60
40
20
0
95
10
5
68
70
72
74
76
78
77
75
Latitude, °S
Latitude, °S
Sea-salt particles with Cl
Modified sea-salt particles without Cl
Minerals + sea-salts
Minerals + sulfates
CaSO4
Sulfates cotaining K
Soot (External)
Sulfates (External)
Sulfates containing Mg

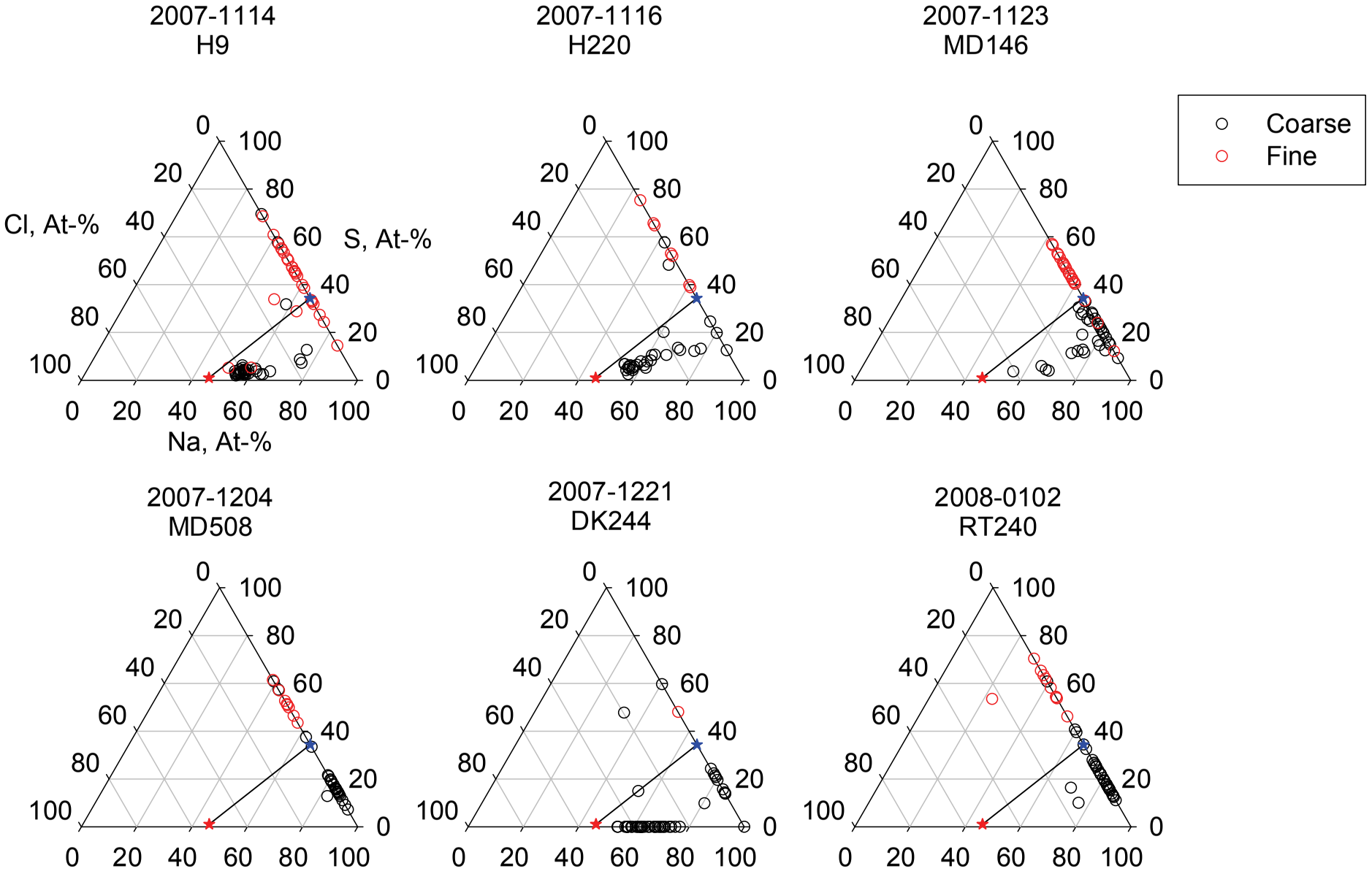
2007-1114
H9
2007-1116
H220
2007-1123
MD146
2007-1204
MD508
2007-1221
DK244
2008-0102
RT240
Cl, At-%
S, At-%
Na, At-%
0
20
40
60
80
100
Coarse
Fine

Fig. 10

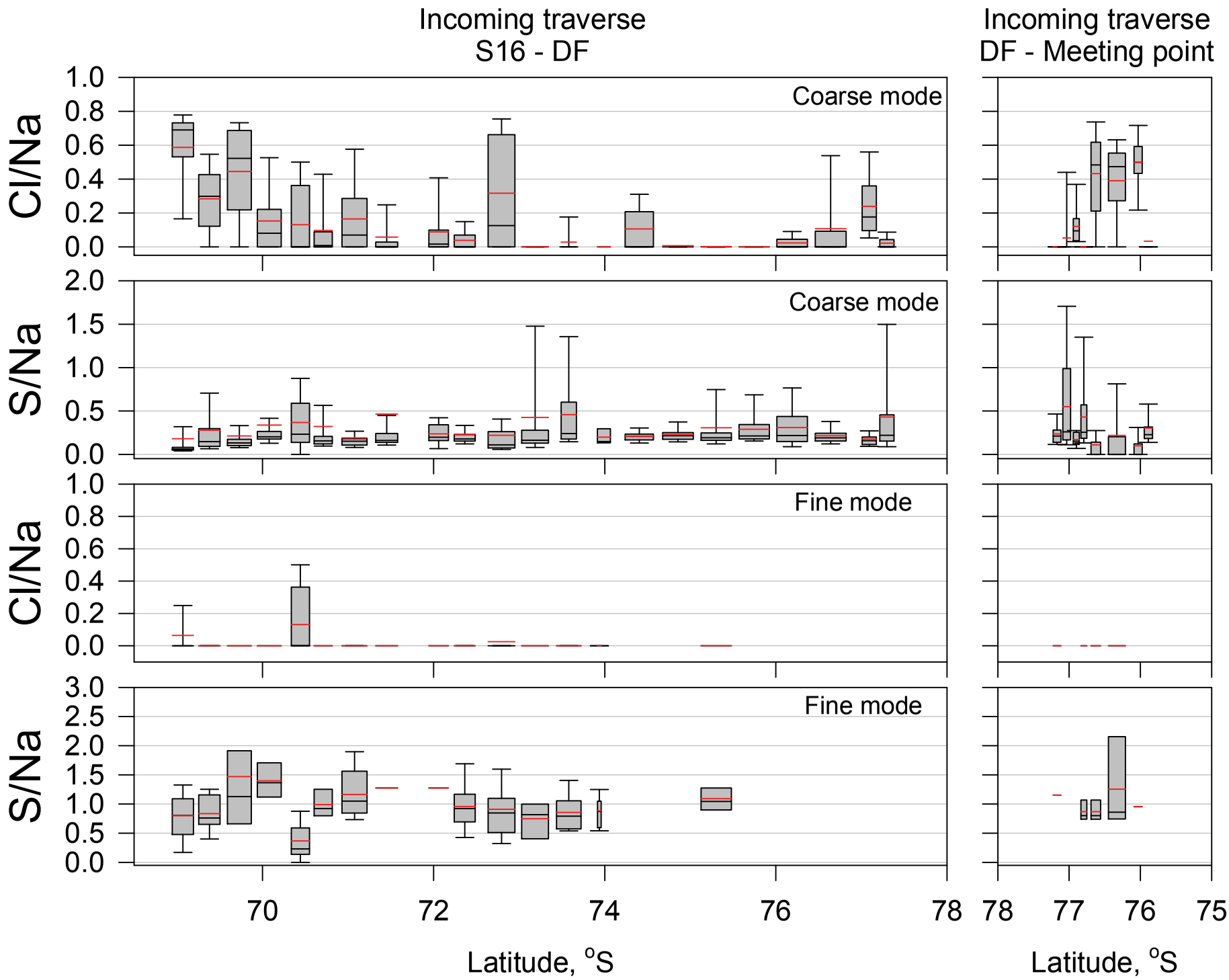
Incoming traverse
S16 - DF
Incoming traverse
DF - Meeting point
Cl/Na
S/Na
Cl/Na
S/Na
Coarse mode
Coarse mode
Fine mode
Fine mode
1.0
0.8
0.6
0.4
0.2
0.0
2.0
1.5
1.0
0.5
0.0
1.0
0.8
0.6
0.4
0.2
0.0
3.0
2.5
2.0
1.5
1.0
0.5
0.0
70
72
74
76
78
78
77
76
75
Latitude, °S
Latitude, °S

Fig.11

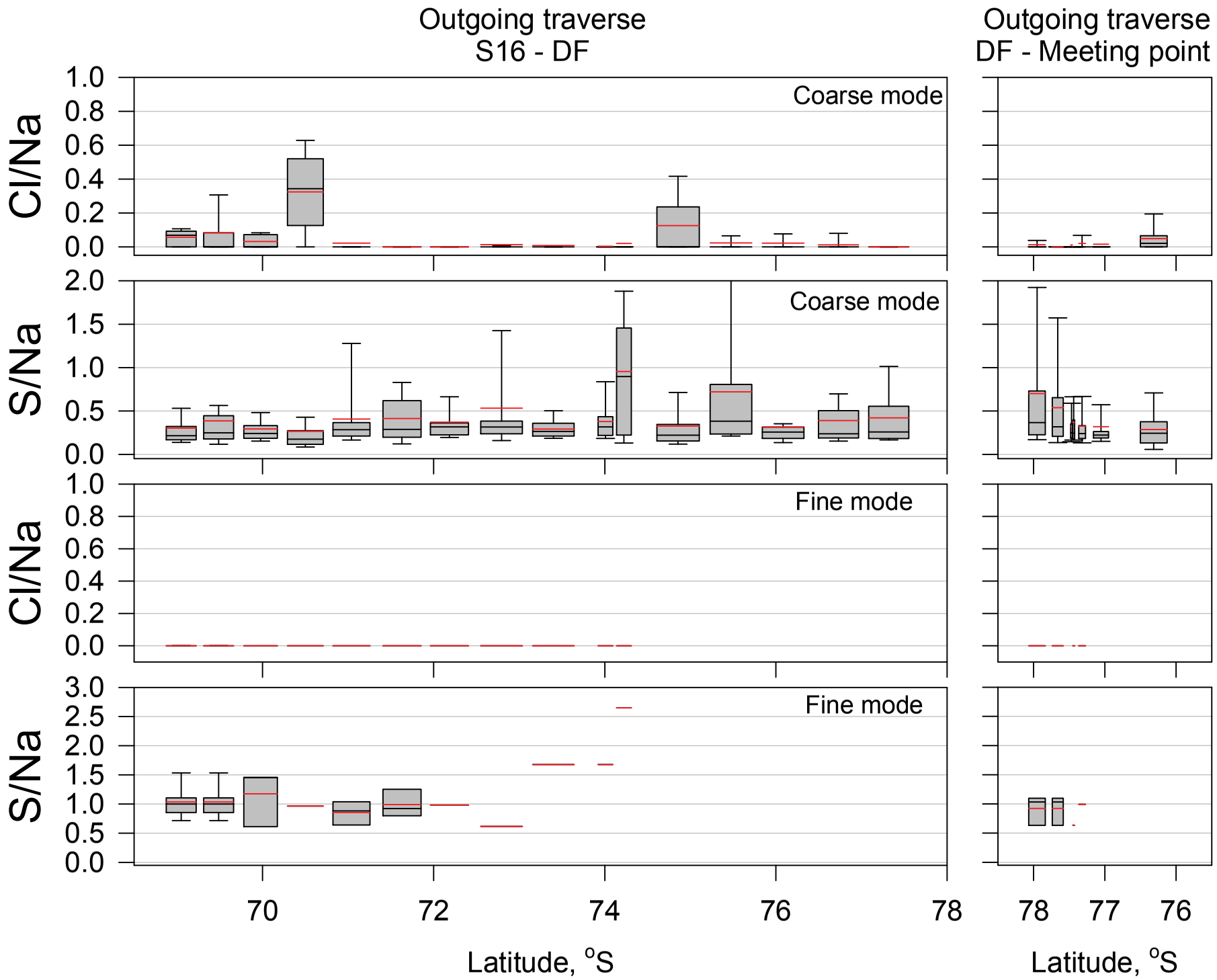
Outgoing traverse
S16 - DF
Outgoing traverse
DF - Meeting point
Cl/Na
S/Na
Cl/Na
S/Na
Coarse mode
Coarse mode
Fine mode
Fine mode
1.0
0.8
0.6
0.4
0.2
0.0
2.0
1.5
1.0
0.5
0.0
3.0
2.5
2.0
1.5
1.0
0.5
0.0
70
72
74
76
78
78
77
76
Latitude, °S
Latitude, °S

Fig.12

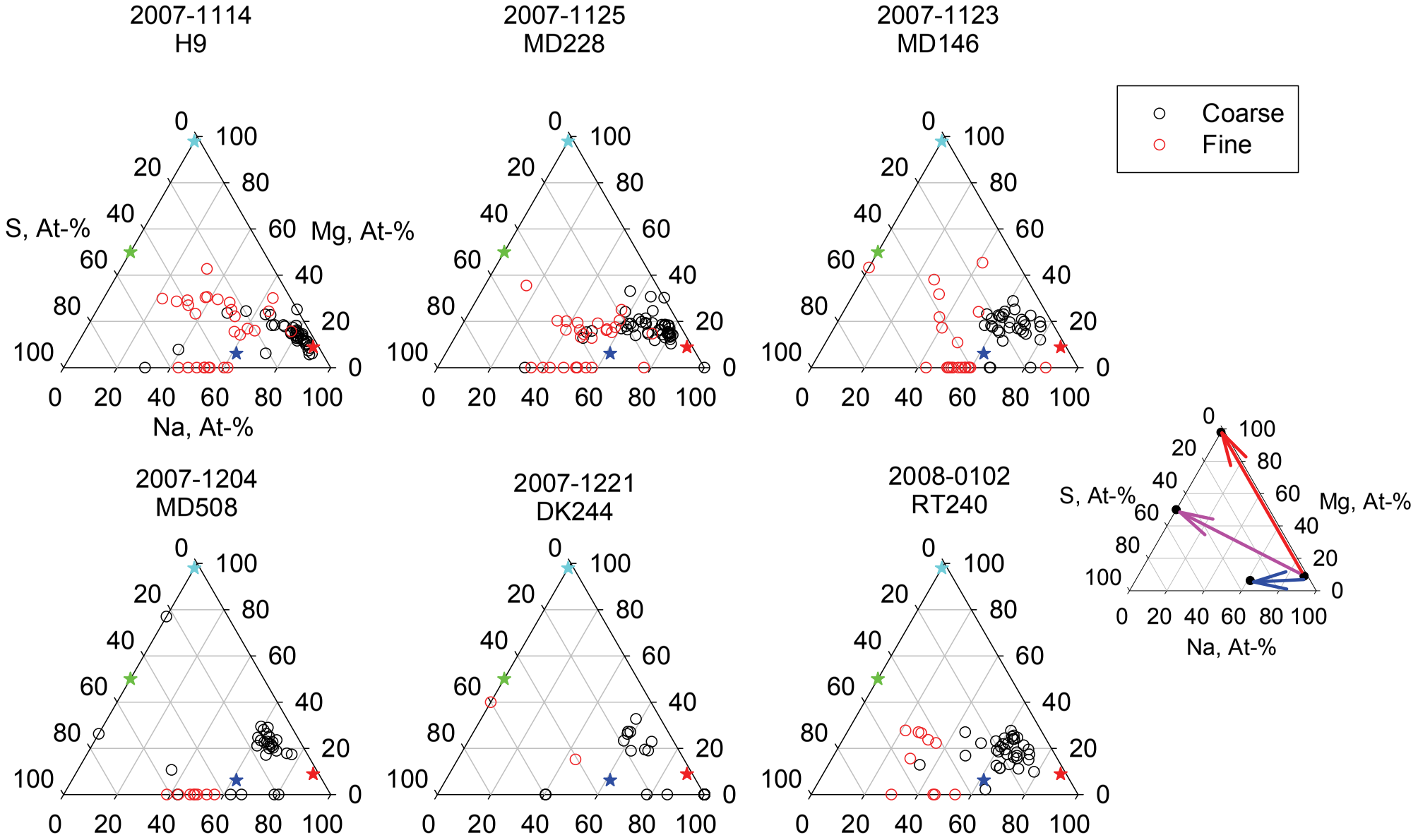
2007-1114
H9
2007-1125
MD228
2007-1123
MD146
Coarse
Fine
S, At-%
Mg, At-%
Na, At-%
2007-1204
MD508
2007-1221
DK244
2008-0102
RT240
S, At-%
Mg, At-%
Na, At-%

Fig.13

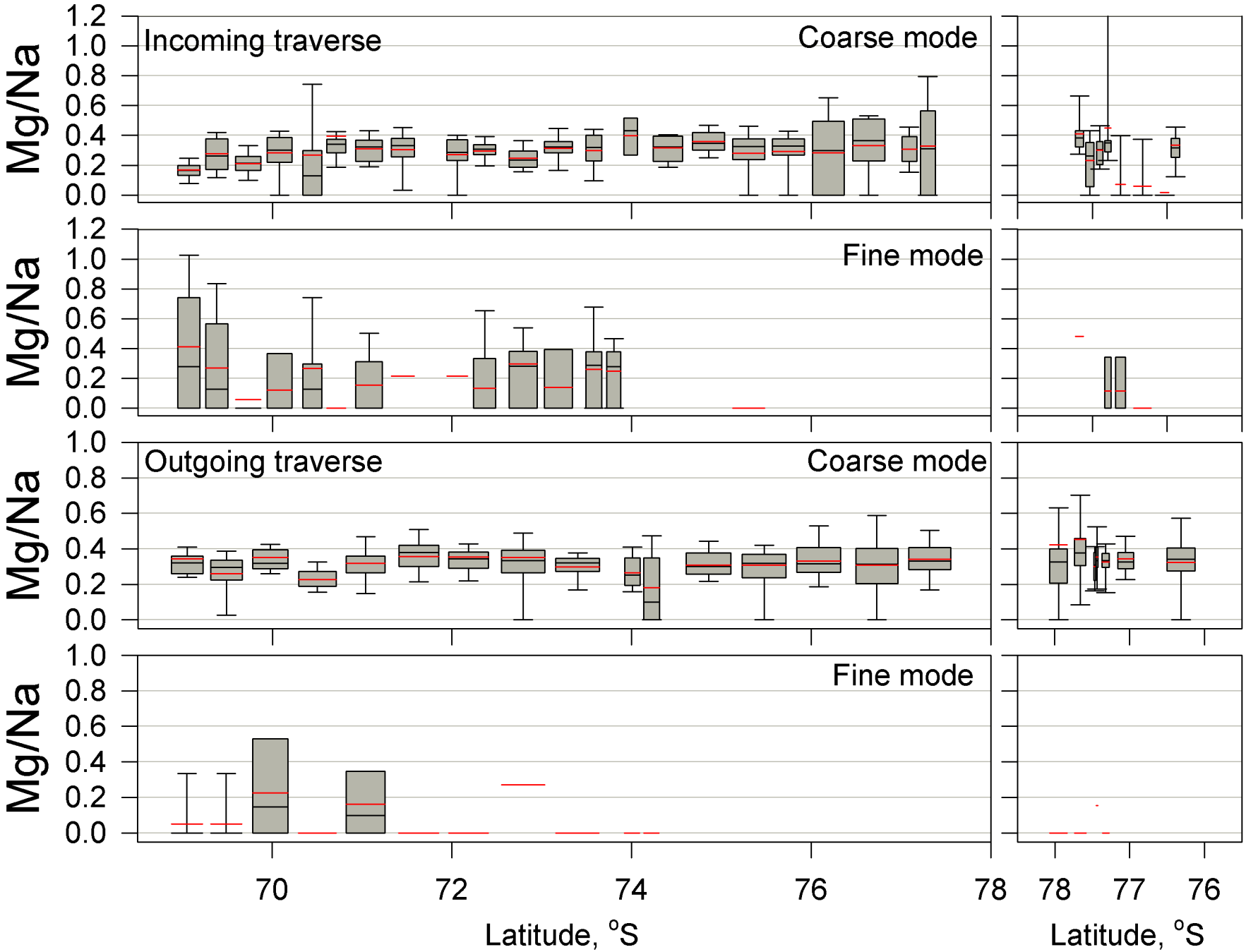
Incoming traverse
Coarse mode
Fine mode
Outgoing traverse
Coarse mode
Fine mode
Mg/Na
1.2
1.0
0.8
0.6
0.4
0.2
0.0
70
72
74
76
78
78
77
76
Latitude, °S
Latitude, °S

fig. 14